remote sensing

Article

Patterns of Typical Chinese Urban Agglomerations Based on Complex Spatial Network Analysis

Sijia Li [1,2,3], Huadong Guo [2,3], Zhongchang Sun [2,3,4,*], Zongqiang Liu [5], Huiping Jiang [2,3] and Hongsheng Zhang [6]

1 College of Mathematics and Physics, Chengdu University of Technology, Chengdu 610059, China
2 International Research Center of Big Data for Sustainable Development Goals (CBAS), Beijing 100094, China
3 Key Laboratory of Digital Earth Science, Aerospace Information Research Institute (AIR), Chinese Academy of Sciences (CAS), Beijing 100094, China
4 Key Laboratory for Earth Observation of Hainan Province, Hainan Research Institute, Aerospace Information Research Institute (AIR), Chinese Academy of Sciences (CAS), Sanya 572029, China
5 State Key Laboratory of Space-Ground Integrated Information Technology, Beijing Institute of Satellite Information Engineering, Beijing 100194, China
6 Department of Geography, The University of Hong Kong, Hong Kong 999077, China
* Correspondence: sunzc@aircas.ac.cn

Abstract: The two prerequisites for monitoring SDG11.A "support positive economic, social and environmental links between urban, peri-urban and rural areas by strengthening national and regional development planning" are the classification of the urban–rural continuum and the extraction of spatial links. However, the complexity and diversity of urban patch distribution make it difficult to achieve a global rapid assessment. Based on the self-developed high-resolution global impervious surface area 2021 (Hi-GISA 2021) product, this study combined the complex network with remote sensing technology to propose a new method to delineate and evaluate the pattern and inner spatial links of the urban–rural continuum for five typical urban agglomerations in China, including the Beijing–Tianjin–Hebei urban agglomeration (BTHUA), the Yangtze River Delta urban agglomeration (YRDUA), the Greater Bay Area (GBAUA), the Chengdu–Chongqing urban agglomeration (CYUA), and the Middle Reaches of Yangtze River urban agglomeration (MRYRUA). The research results are in good agreement with Chinese government documents. First, the five urban agglomerations are all small-world networks with a low degree of overall polycentricity, and the urbanization degrees of GBAUA and YRDUA are higher than BTHUA, CYUA, and MRYRUA. Second, the imbalanced development of YRDUA is higher than the other regions, and the siphon effects of BTHUA and MRYRUA are more significant than YRDUA, CYUA, and GBAUA. Third, some multi-centers show significant siphon effects. The urbanization degree is highly correlated with the urbanization potential but not positively correlated with the degree of balanced development. The results can provide data, methods, and technical support for monitoring and evaluating SDG11.A.

Keywords: urban spatial structure; urban agglomeration; complex spatial network; impervious surface area; urban–rural continuum; urban multi-center; SDG 11

Citation: Li, S.; Guo, H.; Sun, Z.; Liu, Z.; Jiang, H.; Zhang, H. Patterns of Typical Chinese Urban Agglomerations Based on Complex Spatial Network Analysis. *Remote Sens.* **2023**, *15*, 920. https://doi.org/10.3390/rs15040920

Academic Editor: Hua Liu

Received: 30 November 2022
Revised: 14 January 2023
Accepted: 4 February 2023
Published: 7 February 2023

1. Introduction

For the benefit of all people and the planet, rapid global urbanization should be premised on sustainable development. Achieving the sustainable development of global cities is becoming one of the urgent issues to which countries and regions around the world pay close attention [1,2]. The 11th goal of the 17 Sustainable Development Goals (SDGs) proposed by the United Nations (UN) is dedicated to making cities and human settlements inclusive, safe, resilient, and sustainable [3]. According to UN estimates, global urbanization will continue accelerating in the next 30 years [4]. It is expected that from 2021 to 2050, the world urbanization rate will increase from 56% to 68%, and nearly 90% of the growth will occur in developing countries in Asia and Africa. Particularly, China is undergoing an unprecedented process of urbanization [5,6]. By 2030, it is expected that China's urban population will increase by about 200 million inhabitants, and the proportion of the urban population will reach 73% [7]. The rapid development of global urbanization has not only brought about rapid economic growth worldwide, but also caused urbanization problems such as the loss of cultivated land, an increase in urban surface runoff, urban waterlogging, the urban heat island effect, and surface subsidence [8,9]. Therefore, it is necessary to monitor the sustainable development of global urban areas to achieve SDG11, and SDG11.A is committed to "support positive economic, social and environmental links between urban, peri-urban and rural areas by strengthening national and regional development planning" [10]. To overcome the lack of a unified definition and precise measurement of urban composition, based on the links of urban patches, the "urban–rural continuum" has been taken as a new perspective in SDG11.A wherein settlements are divided into urban, peri-urban/semi-dense areas, and rural areas to accurately measure the degree of sustainable development and regional development. There are two prerequisites for monitoring SDG11.A: (1) the mining of the pattern of the urban–rural continuum, that is, the classification and extraction of the urban–rural continuum—urban areas, peri-urban/semi-dense areas, and rural areas; and (2) spatial links should be extracted as baseline reference data to achieve the purpose of strengthening economic, social, and environmental links. However, there are currently no uniform methods and rules for the rapid monitoring and evaluation of the spatial classification and spatial correlation of the urban–rural continuum, especially on a large scale, such as urban agglomerations or globally.

Currently, urban agglomerations, considered an important spatial type in the post-globalization and digitalization era, are the highest form of spatial organization in the mature stage of urban development, manifesting large, polycentric, and multilevel characteristics by geographical correlation [11,12]. The coordinated development of urban agglomerations is a prerequisite for the healthy and efficient sustainable development of global urban areas, which aims to form an integrated pattern that large cities, small- and medium-sized cities, small towns, and villages develop to their full potential to improve regional accessibility, reduce urban communication costs, and improve resource allocation efficiency along with economic vitality. Thus, focusing on SDG11.A to monitor and evaluate the sustainable development of urban agglomerations is an important means to monitor the sustainable development of global urban areas.

Nowadays, the incredible complexity of network structures is becoming the manifestation of urban agglomerations. The complex network is a method to evaluate the links between objects from a global perspective, where different nodes correspond to different objects and edges established between nodes measure connectivity properties. Due to capabilities such as the exploration of big data and the attention to spatial links, the complex network is particularly suitable for remote sensing and geoscience analysis [13]. Since the 1990s, the development of network research in social sciences [12] has prompted planners and geographers to conduct urban network research on different spatial scales [14,15]. Taylor built the Globalization and World Cities Research Network based on enterprise connectivity [16,17]. After that, the types of links of urban networks have gradually expanded into social and cultural links [18,19], traffic links [20], business links [21,22], etc. Thus, for a long time, the complex network has been used to discover links in a range of research, including ecological landscape systems [23,24], hydrological systems [25–27], atmospheric systems [28,29], traffic systems [30,31], virus transmission [32], social information dissemination [33], seismic activity [34], and other systems with connectivity and spatial link characteristics.

One of the premises of monitoring SDG11.A is to extract the spatial links as baseline data, since the feature of the urban agglomeration network is the spatial links between urban patches, which converge to form different spatial patterns. The spatial correlation between links drives the development of spatial patterns. Thus, the development of spatial patterns (i.e., urbanization potential) should be explored from the perspective of spatial correlation.

Tobler's First Law of Geography states that "Everything is related to everything else, but near things are more related to each other"; geographical objects or attributes are related to each other in a spatial distribution, and there are different patterns of agglomeration and random and regular distributions [35]. Thus, the research on the regional urban sustainable development of urban agglomerations should include a joint analysis of spatial correlation and differentiation characteristics. Most of the prior urbanization studies just focused on the characteristics of spatial differentiation, which have summarized urban spatial differentiation models such as concentric circles, multi-cores, and sectors through a large number of cases, and urban expansion models such as infill, edge expansion, and enclave [36–38]. From the expansion of the horizontal and vertical dimensions, they can be summarized as stable expansion, high-speed horizontal expansion, stable vertical expansion, emerging non-structural change, and high-speed vertical expansion [39]. For correlation analysis, the traditional method, which is based on the independent hypothesis of samples, is mainly used to quantitatively describe the common trend of different data, such as Person, Spearman, Kendall coefficient, etc., which are not applicable to the analysis of geospatial objects with spatial autocorrelation characteristics. The study of spatial correlation mainly reflects the aggregation mode of geographical objects [40]. Indicators for calculating global spatial correlation include Moran's I, Geary's C, Getis's G, and Join Count [41]. Indicators for calculating local spatial correlation include Local Moran's I, LISA (Local Indicators of Spatial Association) [42], and Getis's Gi* [41]. Spatial correlation has been widely used in the fields of ecological environment [43,44], plate movement [45,46], and other fields. In the field of urban spatial correlation research, some authors conduct pattern discovery based on the GPS tracking data of population flow to find the correlation between different geographical regions [47,48] and find the hidden connection between urban regions by analyzing the frequent population density changes [49].

Currently, the research on urban spatial correlation is mainly based on the original data, not on the relationship. Most of the data sources for the study of the urban networks' internal links focus on statistical data such as socio-economic and population data, as well as dynamic flow data such as social platform information flow and traffic flow. However, due to the low spatial resolution and real-time lag, it is a challenge to decompose the statistical data into different spatial scales for urbanization analysis. Since the urban spatial pattern can be defined as an "abstract or generalized description of phenomenon distribution in geographic space" [50,51], urban remote-sensing information with a high spatial and temporal resolution can be used to address this problem [52]. Currently, relatively few large-scale urbanization studies based on remote-sensing information have been performed. There still exist two major challenges for global urbanization analysis: (1) the generation of global urban products based on remote sensing images; and (2) the rapid extraction of the spatial aggregation and correlation of global urban patches. Fortunately, many satellite-derived products of global impervious surface area or human settlement have been generated during the last decade, such as FROM-GLC, ESA WorldCover, ESRI Land Use/Land Cover, Hi-GISA, and DYNAMICWORLD, based on Sentinel imagery; GlobeLand30, NUACI, GAUD, and GISA, based on Landsat data; WSF-2015, GAIA, and MSMT-RF, based on Sentinel + Landsat data; MODIS 500, based on MODIS 463-m data; GHS-BUILT, based on global remote sensing data streams, census data, and crowd/volunteered geographic information sources; NLCD, based on Envisat-MERIS; CLC, based on IRS Resourcesat 1/2, SPOT 4/5, and RapidEye constellation; and GUF, based on TerraSAR-X data and TanDEM-X data [53]. Although a few large-scale urbanization spatial pattern analyses have been carried out based on these global products, they are mostly focused on information theory and fractal theory to analyze the attributes and geometric characteristics of urban patches, e.g., the area, perimeter, area density, and shape, resulting in a failure to quantitatively reflect the local and global spatial correlation [54]. The combination of global impervious surface area products and the complex network can quickly identify key nodes or regions of urbanization, excavate the local and global spatial correlation and aggregation, and provide a rapid, intuitive, and interactive analysis tool for urbanization studies. In this study, the complex spatial network and global impervious products are combined to analyze the urbanization of typical urban agglomerations in China. As the five major urban agglomerations in China, the Beijing–Tianjin–Hebei urban agglomeration (BTHUA), the Yangtze River Delta urban agglomeration (YRDUA), the Greater Bay Area (GBAUA), the Chengdu–Chongqing urban agglomeration (CYUA), and the Middle Reaches of Yangtze River urban agglomeration (MRYRUA) have typical urban agglomeration characteristics of spatial correlation and differentiation. To accurately identify and evaluate their spatial pattern, a Hi-GISA 2021-based complex spatial network model, combining complex network and remote sensing technology, is constructed in this study. Firstly, the network model type of urban agglomerations is determined. Secondly, the three major constituent structures of urban agglomerations, i.e., the multi-centers, urban–rural continuums, and urban agglomeration corridors, are extracted and analyzed by spatial correlation. Finally, the balance degree of urbanization and the corresponding regional urbanization potential are further evaluated based on spatial correlation.

The academic contribution of this study is to provide a new method for monitoring SDG11.A. Specifically, the complex network and remote sensing technology are combined to rapidly and accurately map and analyze the pattern and urbanization potential area of China's typical urban agglomerations at a large scale based on the spatial links and the spatial correlations between the links. The research results can provide baseline data for the monitoring of SDG11.A, including the data of multi-center patterns, rural–urban continuum patterns, and urban agglomeration corridor patterns of China's typical urban agglomerations, which is the extraction and mapping of spatial links—global importance, global intermediary—and the data of spatial correlation and urbanization potential area of China's typical urban agglomerations, which is the extraction and mapping of spatial aggregation patterns of spatial links, called spatial correlation. The results can accurately assess the urbanization development status of these urban agglomerations and provide data, methods, and technical support for monitoring and evaluating "SDG11.A", to "support positive economic, social and environmental links between urban, peri-urban and rural areas by strengthening national and regional development planning".

2. Study Area and Dataset

2.1. Study Area

BTHUA, YRDUA, GBAUA, CYUA, and MRYRUA are the five growth poles of China's urban agglomerations that act as multi-center engines to promote high-quality regional development. Specifically, Beijing is regarded as the center to lead the development of BTHUA, and Shanghai is considered the center of YRDUA. GBAUA has multiple central cities, including Hong Kong, Macau, Guangzhou, and Shenzhen; CYUA has Chongqing and Chengdu; and MRYRUA has Wuhan, Changsha, Nanchang, and Hefei. The spatial distribution of these urban agglomerations is shown in Figure 1.

2.2. Dataset

This study uses China's product extracted from the Hi-GISA 2021, a self-produced global 10 m-resolution high-precision impervious surface product (Figure 2). Hi-GISA 2021 utilizes multi-temporal up-and-down orbit Sentinel-1 SAR and Sentinel-2 MSI multispectral optical data combined with scattering features, texture features, and phenological features to conduct global 10 m-resolution impervious surface extraction and updating, and the resultant accuracy is better than 88.00% [53,55].

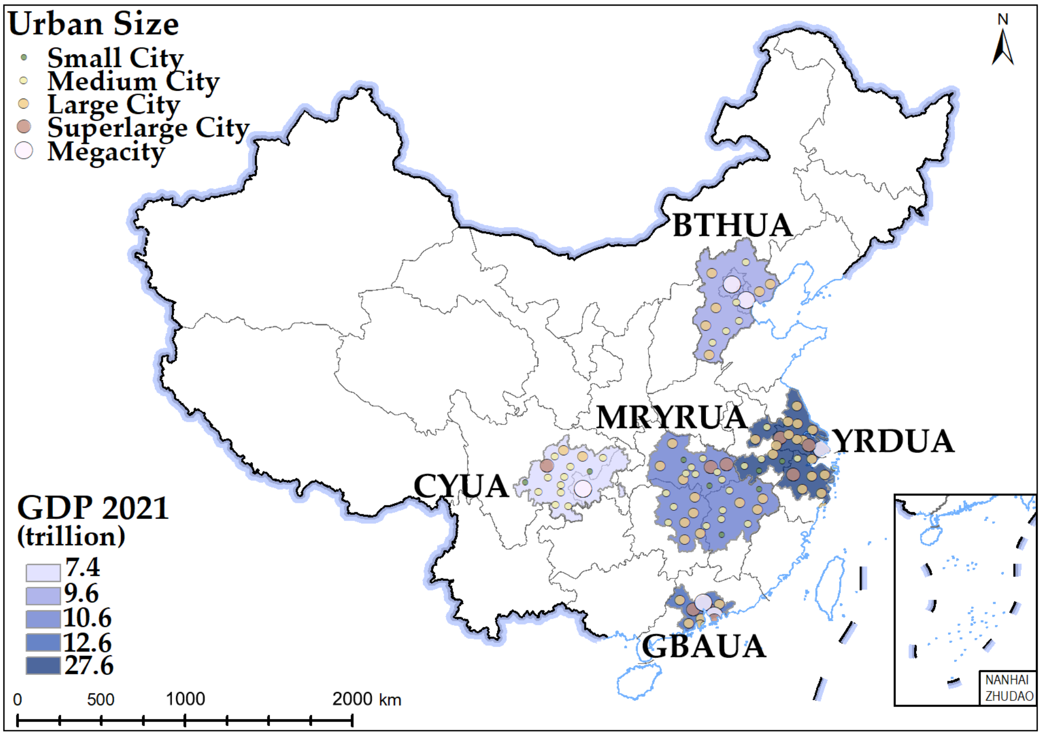

Figure 1. Spatial distribution of BTHUA, YRDUA, GBAUA, CYUA, MRYRUA. Megacity: the permanent urban population is more than 10 million. Super-large city: the permanent urban population is 5 to 10 million. Large city: the permanent urban population is 1 to 5 million. Medium city: the permanent urban population is 500,000 to 1 million. Small city: the permanent urban population is less than 500,000.

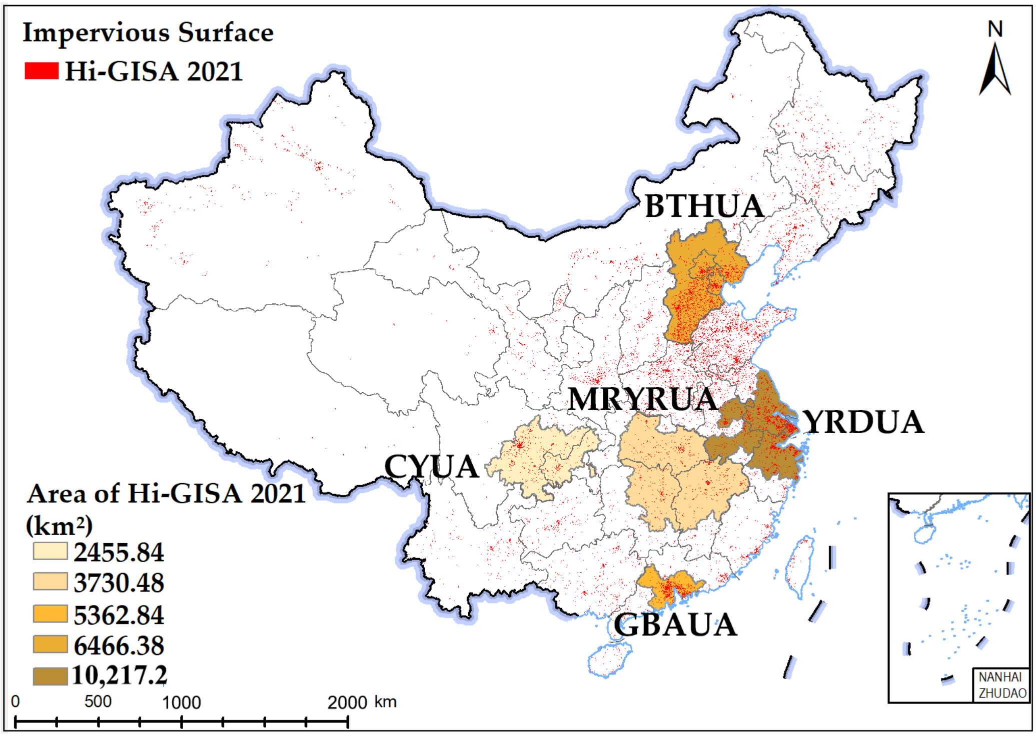

Figure 2. Spatial distribution of China's impervious surfaces from Hi-GISA 2021.

3. Methods

Based on Hi-GISA 2021, this study combines complex network analysis with remote sensing technology to build a complex spatial network model of urban agglomerations, aiming to perform the analysis of spatial correlation and differentiation for large-scale urban agglomerations. The research is mainly divided into three stages, and Figure 3 shows the work flow.

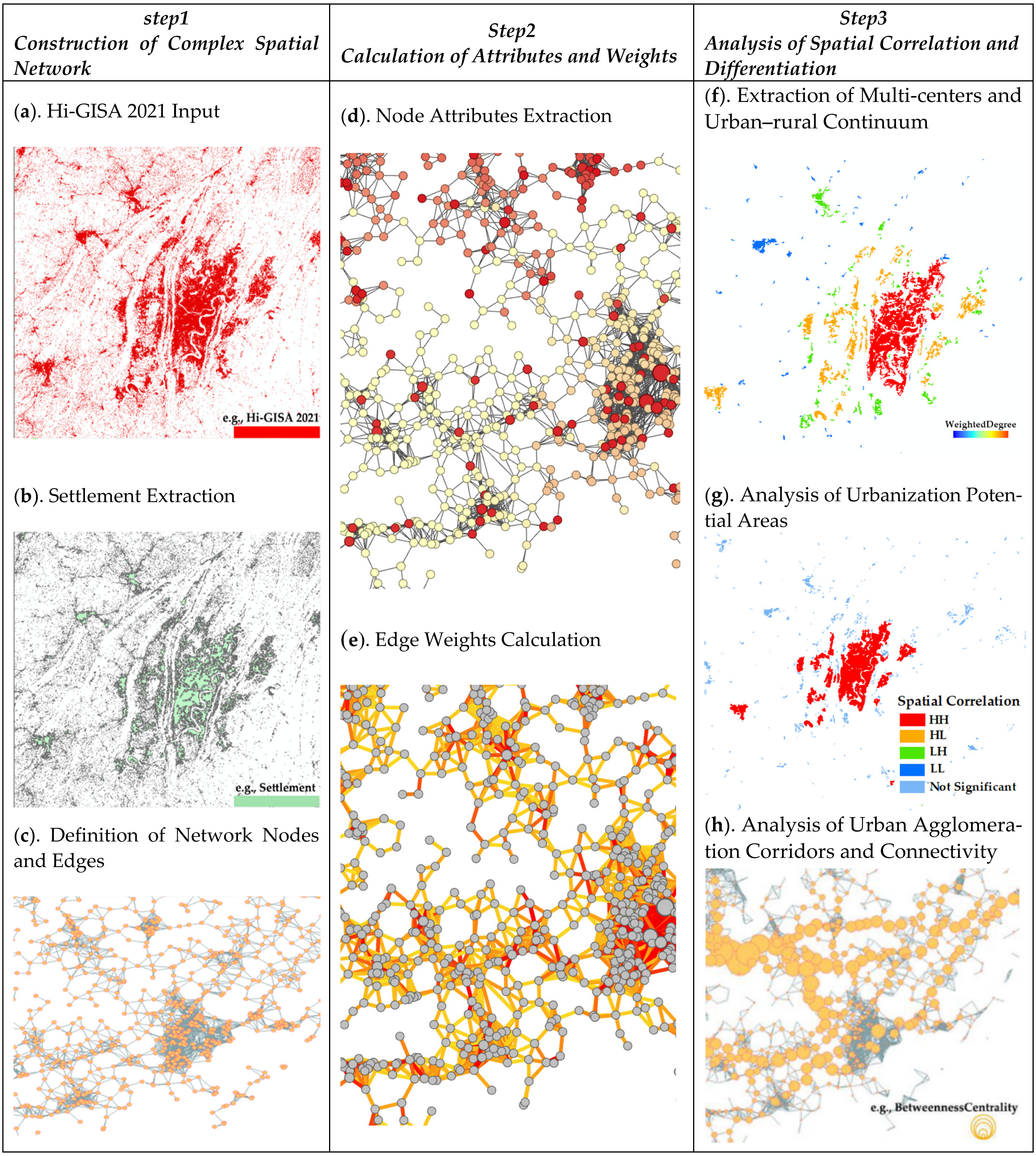

Figure 3. Flow chart of the complex spatial network analysis of urban agglomerations.

(1) First, we use the residential points extracted from Hi-GISA 2021 to construct the corresponding complex spatial networks of urban agglomerations. The network nodes correspond to the centroid of the settlement, and the undirected edges established between nodes in a buffer zone represent a measurement of connectivity properties;
(2) Second, the attributes of nodes and the weights of edges are simultaneously calculated;
(3) Finally, we construct evaluation indicators, calculate the correlation and importance of nodes, and compare the multi-centers, urban–rural continuums, urban agglomeration corridors, and connectivity. Meanwhile, we further evaluate the degree of urbanization balance and urbanization potential of urban agglomerations.

3.1. Complex Spatial Network Attribute Extraction and Weight Calculation

3.1.1. Node Attributes Extraction

The most commonly used geometric properties of shapes are area and perimeter. The indicator of area refers to the sum of the sizes of all the pixels that make up the geographic shape, and the perimeter attribute represents the sum of the pixel sizes of the outer boundaries of the geographic shape.

3.1.2. Edges Weights Calculation

In this study, an improved spatial proximity model is constructed to extract the spatial proximity of edges as the edge weight for the respective urban agglomeration network.

Spatial proximity: Tobler's First Law of Geography states that the spatial proximity of geographic objects is proportional to the length of the common boundary and inversely proportional to the center distance. It can be calculated as formula (1), where p_{ij} is the spatial proximity of geographic objects i and j, l is the length of the common boundary of i and j, and d_{ij} is the spatial distance between them.

Improved Spatial Proximity Model: In order to better describe the spatial proximity relationship of discrete geographic objects, a simple weighted criterion is constructed based on Formula (1), which is calculated as Formula (2):

$$p_{ij} = l/d_{ij} \tag{1}$$

$$P'_{ij} = A_i A_j^m / d_{ij}^r \tag{2}$$

where P'_{ij} is the improved spatial proximity of discrete geographic objects i and j, A_i and A_j are the areas of i and j respectively, d_{ij} is the Haversine distance between i and j, the Haversine distance was used to calculate the shortest distance on the surface of the earth (treated as a sphere) between two locations with given coordinates [56], m is the attenuation factor of approaching strength between i and j, and r is the friction coefficient (generally m = 0.5, r = 2).

The calculation of edge weights can introduce other geospatial data, such as administrative, river, fault, road, forest cover, mountain, etc. Edges separated by the objects above obtain lower weights. In this study, city administrative boundary data are introduced to reduce the weight of edges spanning different cities.

3.2. Construction of Evaluation Indicators for the Complex Spatial Network

The complex spatial network evaluation indicators of urban agglomerations are shown in Table 1.

Table 1. The evaluation indicators of urban agglomeration complex spatial networks.

Indicators		Definition
Centrality [57]	Weighted degree centrality	The most direct indicator for computing node centrality and importance. The edge a_{ij} connecting nodes i and j has a spatial proximity weight w_{ij}, and the weighted degree of node i is formulated as $\sum_{j \in N} a_{ij} w_{ij}$.
	Betweenness centrality	Measures the frequency with which a node appears on the shortest path in the network, calculated as the ratio of the number of shortest paths passing through the node to the shortest paths in the network. Used to find bridge nodes in the network.
Small-world network characteristics evaluation index [58]	Shortest path	The number of edges that pass through the fewest other nodes among all paths connecting a node pair.
	Clustering coefficient	Describes the degree of clustering between nodes, which refers to the ratio of the actual number of edges between all adjacent nodes to the maximum possible number of edges.
	Average path length	Calculated as the mean of all the shortest paths of the network.
	Average clustering coefficient	Calculated as the mean of the clustering coefficients of all nodes.
	Network diameter	Characterizes the network size, calculated as the maximum value of all shortest paths in the network.
	Small-world evaluation index	Evaluates the strength of small-world features of different networks, calculated as the ratio of the average clustering coefficient to the average path length.
Spatial correlation index [59,60]	Degree distribution	The probability distribution of the node degree. The probability of a node whose degree is k is formulated as P(k) = n(k)/N, where n(k) represents the number of nodes whose degree is k, N is the total number of nodes, and the degree distribution is the overall distribution of P(k).
	Global Moran's I	Calculates whether there is aggregation or abnormal values. Moran's I > 0 means that the data show positive spatial correlation, and the greater the value, the greater the spatial correlation; Moran's I < 0 means that the data show negative spatial correlation, and the smaller the value, the greater the spatial difference; and Moran's I = 0 means the data are random. Positive spatial correlation means that the correlation becomes more significant as the spatial distribution location (distance) gathers. Negative spatial correlation means that the correlation becomes significant with the dispersion of spatial distribution.
	Local Moran's I	Calculates the spatial distribution of clustered or abnormal values.

3.3. Construction of the Complex Spatial Network

The UN Habitat recommends connecting urban land larger than 20 hectares and less than 200 m as the minimum urban land standard [61]. In this study, the qualified Hi-GISA 2021 impervious surface pixels are connected and then clipped by the city boundary to obtain human settlement objects, and the centroids of these objects are extracted as nodes of the network.

Second, buffer processing with a certain buffer radius of outline edges for settlement objects is performed, and the undirected edges established between nodes in the buffer zone are used to measure connectivity properties. Buffering based on the outline edge of the object ensures the real influence range of the actual shape and area of human settlements in the network. Tobler's First Law of Geography states that spatial correlation is the basis for constructing a spatial pattern and is not affected by spatial scale. Although the size of the buffer radius has little effect on spatial correlation evaluation, the smaller the buffer radius, the more the local spatial correlation and aggregation the network can emphasize. Similarly, the larger the buffer radius, the more it can get rid of the redundancy of local information and focus on the global spatial correlation and aggregation. Given the minimum area of the center for China's first-tier cities (15 km^2) [62] and the previous experience of buffer setting (15 km) for the complex spatial network construction of European cities [54], this study sets the buffer radius to 15 km. Finally, the complex spatial networks of BTHUA, YRDUA, GBAUA, CYUA, and MRYRUA are constructed, respectively (Figure 4).

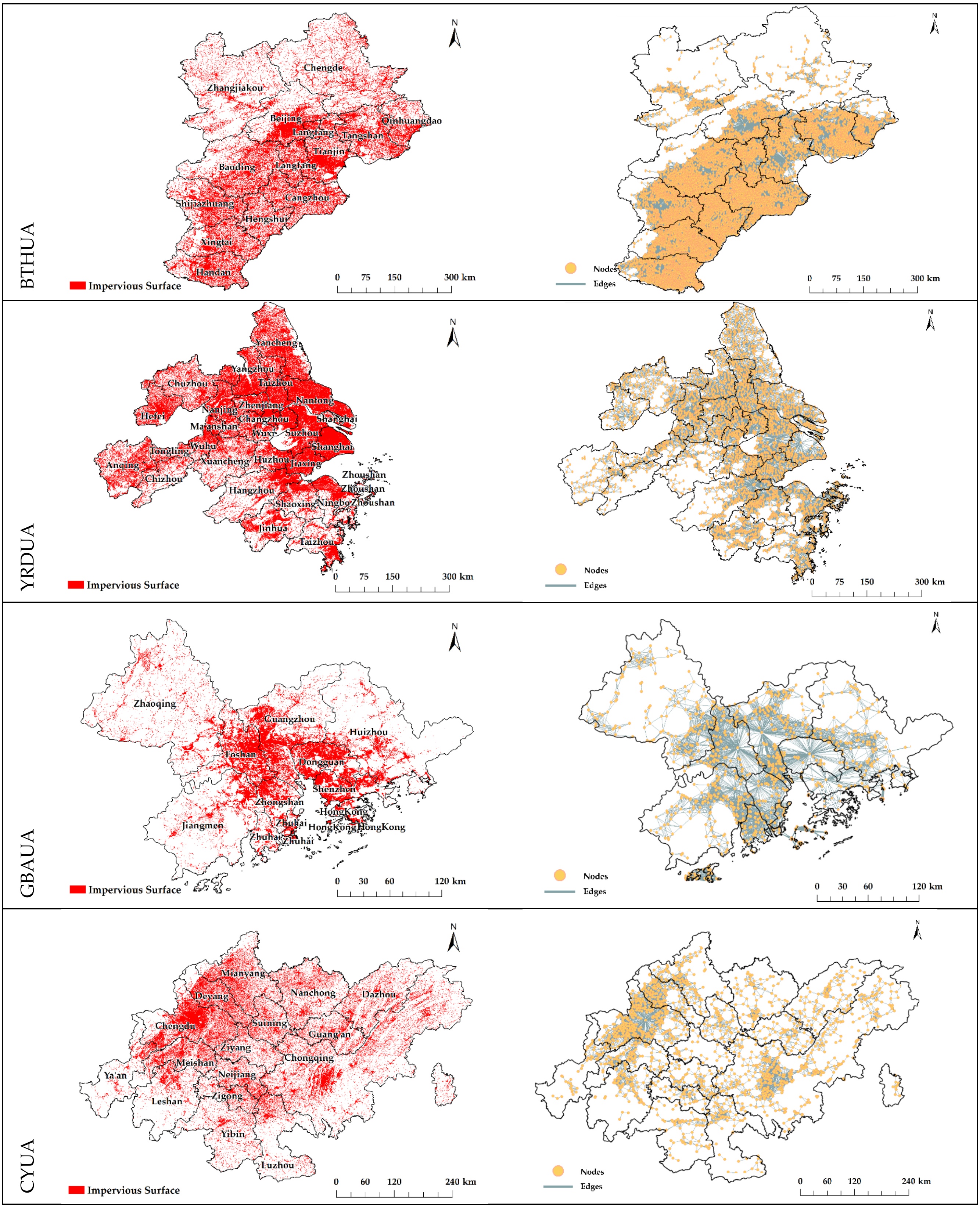

Figure 4. *Cont.*

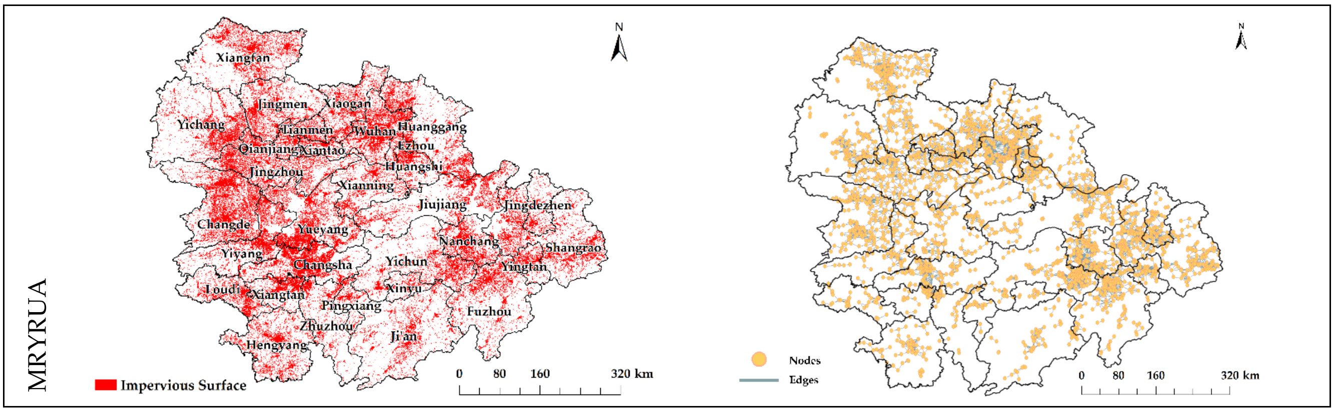

Figure 4. Complex spatial networks of BTHUA, YRDUA, GBAUA, CYUA, and MRYRUA.

4. Results

4.1. Complex Spatial Network of Urban Agglomerations

The complex spatial networks of BTHUA, YRDUA, GBAUA, CYUA, and MRYRUA are constructed as in Figure 4. The red patches represent the impervious surfaces, the yellow network nodes correspond to the centroid of the impervious surfaces, and the gray edge connects the neighbor nodes within the 15 km buffer radius to represent the spatial links. The number of nodes in the BTHUA, YRDUA, GBAUA, CYUA, and MRYRUA networks is 12,963, 4436, 987, 1747, and 2680, and the number of edges is 625,303, 53,827, 10,780, 12,902, and 16,834 respectively.

4.2. Analysis of Spatial Correlation and Differentiation Characteristics of Complex Spatial Networks

4.2.1. Determination of Urban Agglomeration Complex Spatial Networks—Small-World Networks

When the number of nodes is large, the degree of distribution of the small-world network can be approximated to a normal distribution. In this study, the complex spatial network degree distributions of BTHUA, YRDUA, GBAUA, CYUA, and MRYRUA approximately exhibit normal distributions (Figure 5), and the determination coefficients of R^2 for the corresponding fitting functions are 0.93, 0.97, 0.81, 0.88, and 0.92, respectively.

A small-world network is characterized by a small average path length (APL) and a high average clustering coefficient (ACC), which are close to a random network and a regular network (close to 1), respectively. In order to quantify small-world characteristics, the APL and ACC of complex spatial networks for the five urban agglomerations were calculated, and the corresponding Bernoulli random networks were constructed based on the number of nodes and the average degree to obtain the resultant APL and ACC (Table 2). Comparing the two types of networks, the results show that the five urban agglomerations are typical small-world networks. The APL of GBAUA (5.32) is closest to the value of the corresponding random network (2.58), and the ACC is 0.71, which is much larger than 0.0220, the value of the random network. The difference between the APL of the other four urban agglomeration networks and the corresponding random network is between 8 and 12, which is much smaller than the network diameter, and the ACC is two orders of magnitude higher than that of the random network. Furthermore, the small-world evaluation index indicates that GBAUA shows the strongest small-world characteristic, which is one order of magnitude higher than other urban agglomerations. Different types of networks have different characteristics, and in a small-world network, the communication and the spread of viruses have been enhanced. Local behaviors can quickly affect the overall results. Thus, it is necessary to quantitatively monitor and analyze key nodes, such as the multi-center hubs and corridor hubs of urban agglomerations.

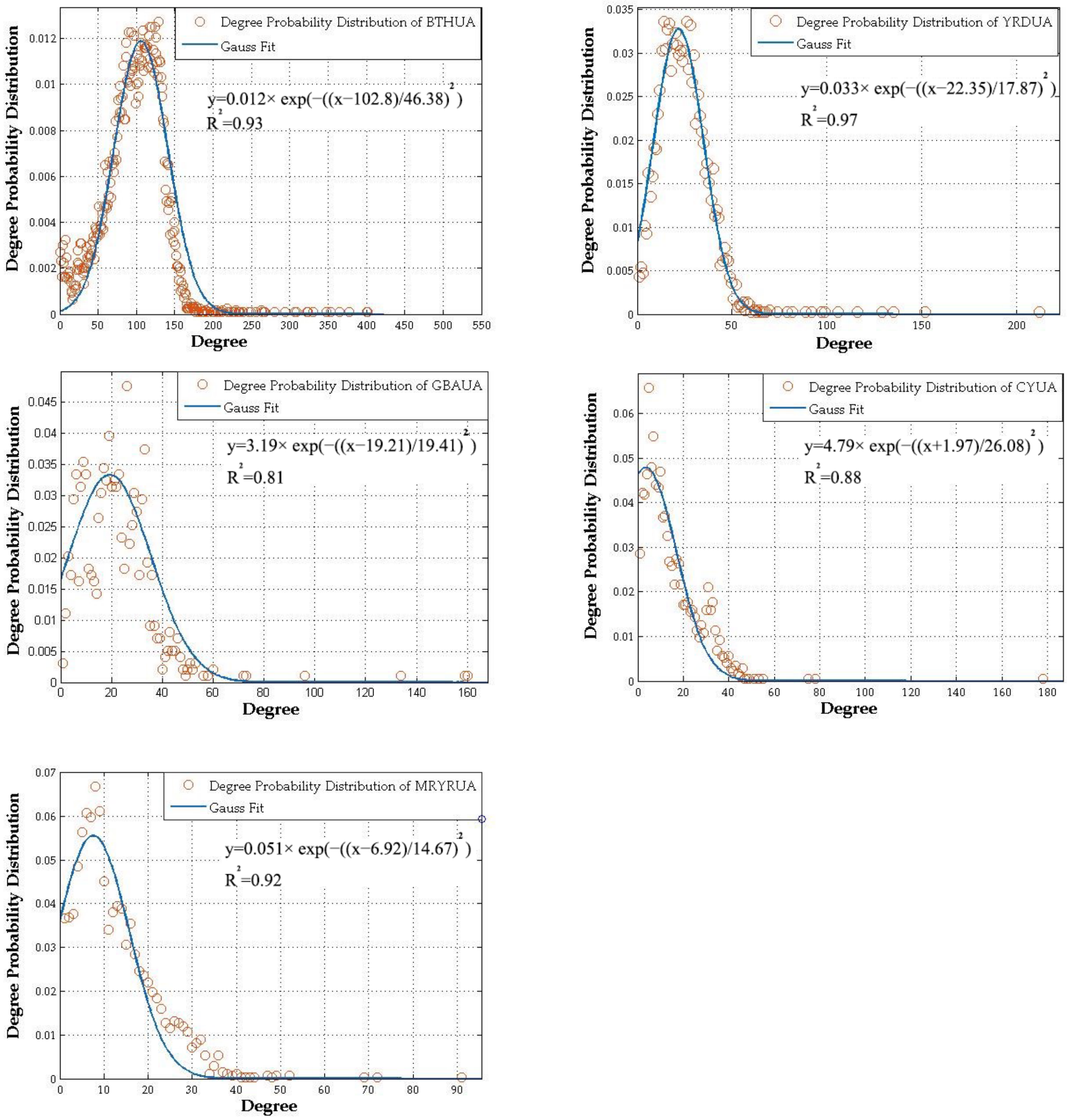

Figure 5. Cumulative probability degree distributions of complex spatial networks for the respective urban agglomerations.

Table 2. Small-world indicators of urban agglomeration complex spatial networks.

Urban Agglomerations	Urban Agglomerations Complex Spatial Networks				Bernoulli Networks	
	Average Path Length	Average Clustering Coefficient	Network Diameter	Small-World Evaluation Index	Average Path Length	Average Clustering Coefficient
BTHUA	10.59	0.63	35	0.06	2.46	0.0074
YRDUA	14.60	0.65	48	0.05	2.91	0.0055
GBAUA	5.32	0.71	16	0.13	2.58	0.0220
CYUA	17.33	0.63	51	0.04	5.00	0.0085
MRYRUA	15.42	0.65	48	0.04	3.42	0.0047

4.2.2. Analysis of Urban–Rural Continuums and Urbanization Potential Areas

(1) Extraction of Multi-centers and Urban–rural Continuums of Urban Agglomerations

The basic feature of an urban agglomeration network is different spatial links that are aggregated to form different spatial patterns. Based on complex spatial network models and indicators, spatial links can be quickly extracted to identify spatial patterns. To extract the urban agglomerations multi-centers and urban–rural continuums, the spatial proximity is used as the edge weights to firstly obtain the node's weighted degree centrality in this study. Second, the complex spatial network-based node weighted degree centrality is constructed (Figure 6a), and the Natural Breaks (Jenks) method is used to grade the color to obtain the multi-centers, which are represented by big red nodes. Last, the urban–rural continuum spatial distribution map based on the weighted degree centrality of impervious surface areas (Figure 6b) is constructed, and the Natural Breaks (Jenks) method is used to grade the color to obtain the urban–rural continuum. The red impervious surface areas represent the multi-centers of the urban agglomerations, orange impervious surface areas represent the city–town area, green represents semi-dense areas, and blue represents rural areas. The red and orange impervious surface areas are collectively referred to as urban areas in this study.

The complex spatial network based on the nodes' weighted degree centrality shows that the numbers of multi-centers for BTHUA, YRDUA, GBAUA, CYUA, and MRYRUA are 10, 12, 8, 2, and 3, respectively (Figure 6a). This suggests that the overall degree of polycentricity in Chinese typical urban agglomerations is relatively low. The five urban agglomeration networks present a variety of dual-core, three-core, and multi-core structures. The multi-core urban agglomerations are located in the eastern plains, while the dual-core and three-core urban agglomerations are located in the mountainous areas in central and western China. The northwest of BTHUA and central CYUA and MRYRUA are lacking multi-centers. However, the multi-center distribution of YRDUA and GBAUA is more balanced.

	(**a**) Complex Spatial Networks Based on Nodes Weighted Degree Centrality	(**b**) The Urban–rural Continuum Spatial Distribution Based on Weighted Degree Centrality of Impervious Surface Areas
BTHUA	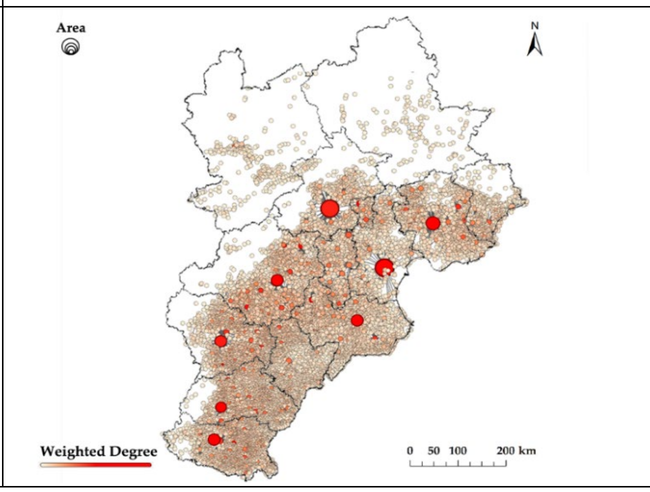	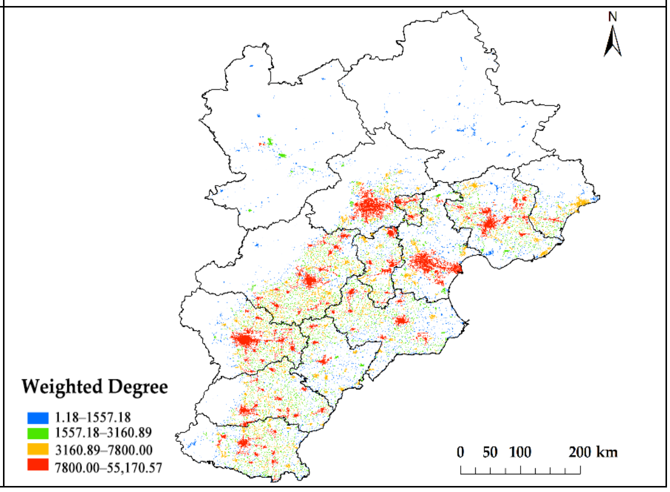

Figure 6. *Cont.*

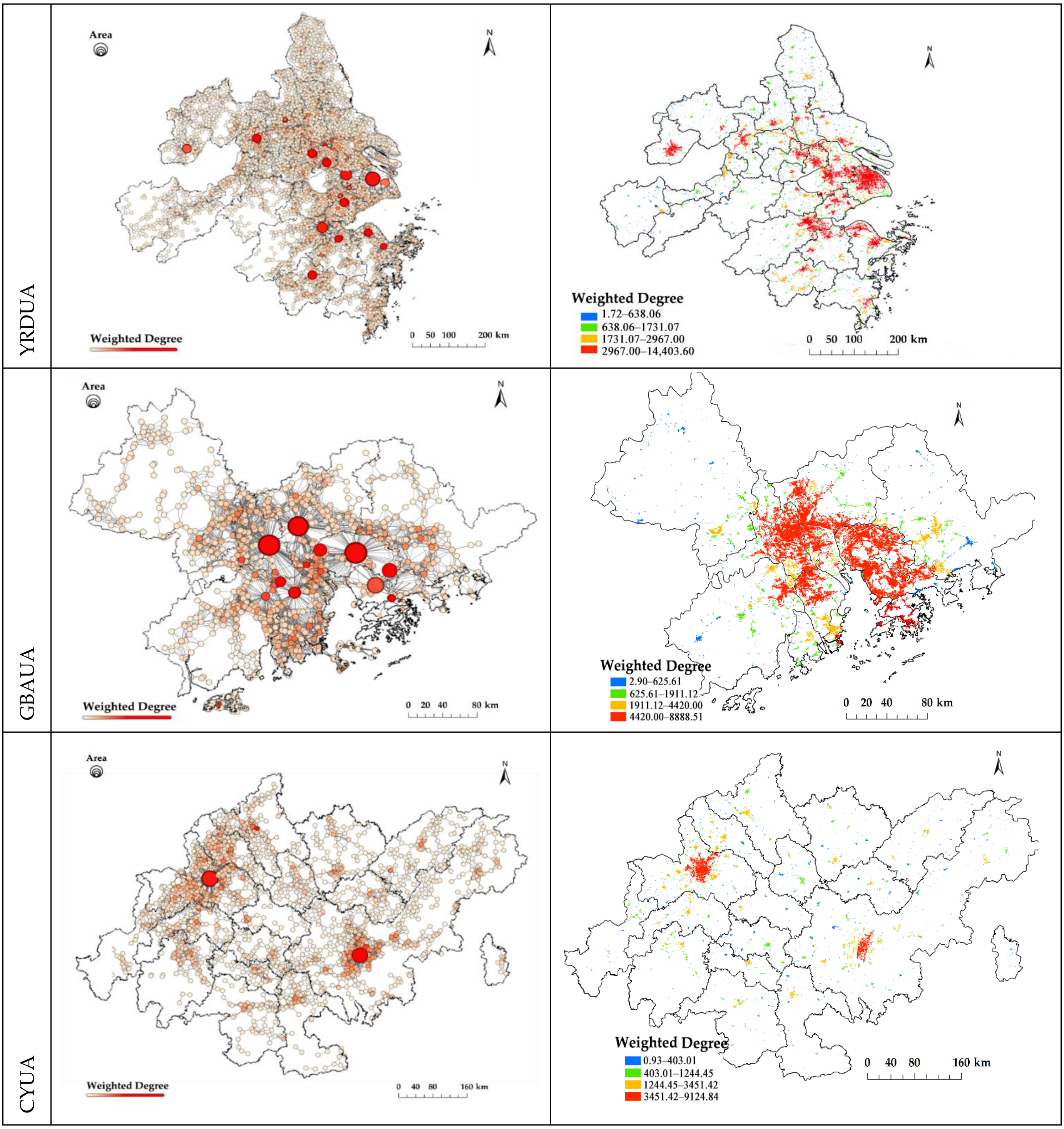

Figure 6. *Cont.*

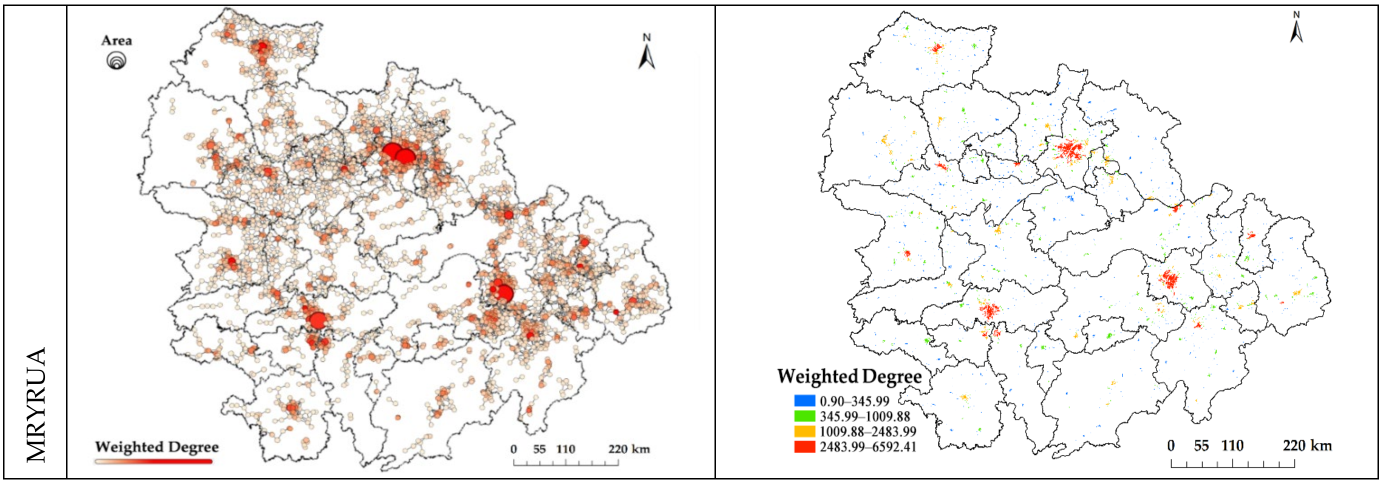

Figure 6. Complex spatial networks and urban–rural continuum spatial distribution based on weighted degree centrality.

Specifically, the multi-centers of BTHUA are located in central and southern Beijing, central Langfang, central and western Tangshan, southeast Baoding, central and southern Tianjin, central Shijiazhuang, central Cangzhou, central Hengshui, southern Xingtai, and central Handan. The multi-centers of YRDUA are located in central Hefei, central Nanjing, eastern Changzhou, northeastern Wuxi, southern Nantong, central Suzhou, central Shanghai, central Jiaxing, northeastern Hangzhou, northern Shaoxing, northern Ningbo, and north of Jinhua. GBAUA's multi-centers are located in central Foshan, southwest Guangzhou, central Dongguan, western Shenzhen, northern Zhongshan, northeastern Jiangmen, and southern Hong Kong. CYUA's multi-centers are located in central Chengdu and western Chongqing. MRYRUA's multi-centers are located in central Wuhan, Changsha, and Nanchang. The urban areas of the five urban agglomerations are mainly distributed around the outer edges of the multi-centers.

The urban–rural continuum spatial distribution map based on the weighted degree centrality of impervious surface areas shows that BTHUA, YRDUA, and GBAUA's urban areas are mainly distributed in the southeast, east, and middle regions, while CYUA is distributed in the east and west, and MRYRUA is distributed in the north, southeast, and southwest (Figure 6b). The semi-dense areas and rural areas of BTHUA, YRDUA, and GBAUA are distributed at the edge of urban areas at a small scale, while CYUA and MRYRUA are widely distributed in the central part.

The urban–rural continuum classification results (Figure 7) show that the percentage of GBAUA's, YRDUA's, BTHUA's, CYUA's, and MRYRUA's urban areas decrease sequentially, at 0.82, 0.71, 0.59, 0.57, and 0.50, respectively. GBAUA has the highest percentage of multi-center areas while MRYRUA has the lowest percentage. The percentage of city–town areas of YRDUA is the highest and GBAUA's is the lowest. The percentage of MRYRUA's semi-dense areas is the highest, and GBAUA's is the lowest. MRYRUA has the highest percentage in rural areas, and GBAUA has the lowest.

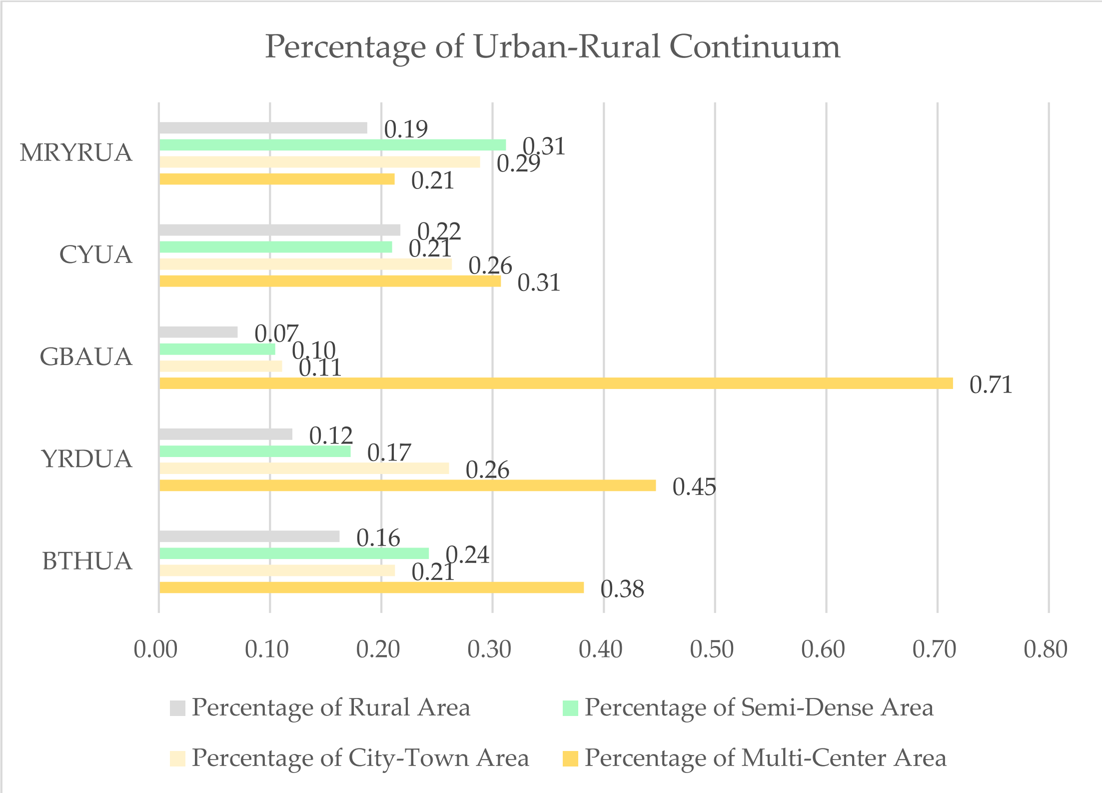

Figure 7. Area percentages of urban–rural continuum classifications.

(2) Analysis of Urbanization Potential Areas

The spatial aggregation pattern among spatial links drives the development of the spatial pattern, so the research on the development potential of the spatial pattern should be based on the global spatial correlation and local spatial correlation. In order to analyze the spatial agglomeration degree of urban agglomerations and evaluate the balance of urbanization, the spatial autocorrelation of weighted degree centrality based on Global Moran's I and local Moran's I is calculated in this study. First, the values of global Moran's I for BTHUA, YRDUA, GBAUA, CYUA, and MRYRUA are calculated based on the inverse distance method with a distance threshold of 15 km, and are 0.0016, 0.1067, 0.0018, 0.0052, and 0.0017 respectively, showing weak positive spatial correlation and aggregation. YRDUA has the strongest aggregation, and BTHUA has the weakest aggregation. Second, based on local Moran's I, the cluster maps for local indicators of association (LISA) are generated to analyze the spatial distribution of the spatial autocorrelation based on the weighted degree centrality of impervious surface areas (Figure 8), and the percentages of spatial correlation classifications are calculated (Figure 9). HH represents a high value surrounded by high values; the weighted degree centrality of the current node and the neighbor nodes 15 km away are both high, highlighting the area with high potential for urbanization. LL is a low-potential area for urbanization, with low values surrounded by low values. HL is a high value surrounded by low values, and the high-value area is siphoning high potential. LH is a low value surrounded by high values, and the low-value area siphons low potential. Overall, the HH and HL areas of BTHUA, YRDUA, GBAUA, CYUA, and MRYRUA are significant in the LISA map while LH and LL areas are not. The HH areas of BTHUA, YRDUA, GBAUA, CYUA, and MRYRUA are located in the central, eastern, central, eastern and western, and eastern and northern parts of the regions, respectively. The HL areas of BTHUA, YRDUA, CYUA, and MRYRUA are mainly distributed in the east, west, northeast, and west, respectively, while the HL of GBAUA is not significant in the LISA map.

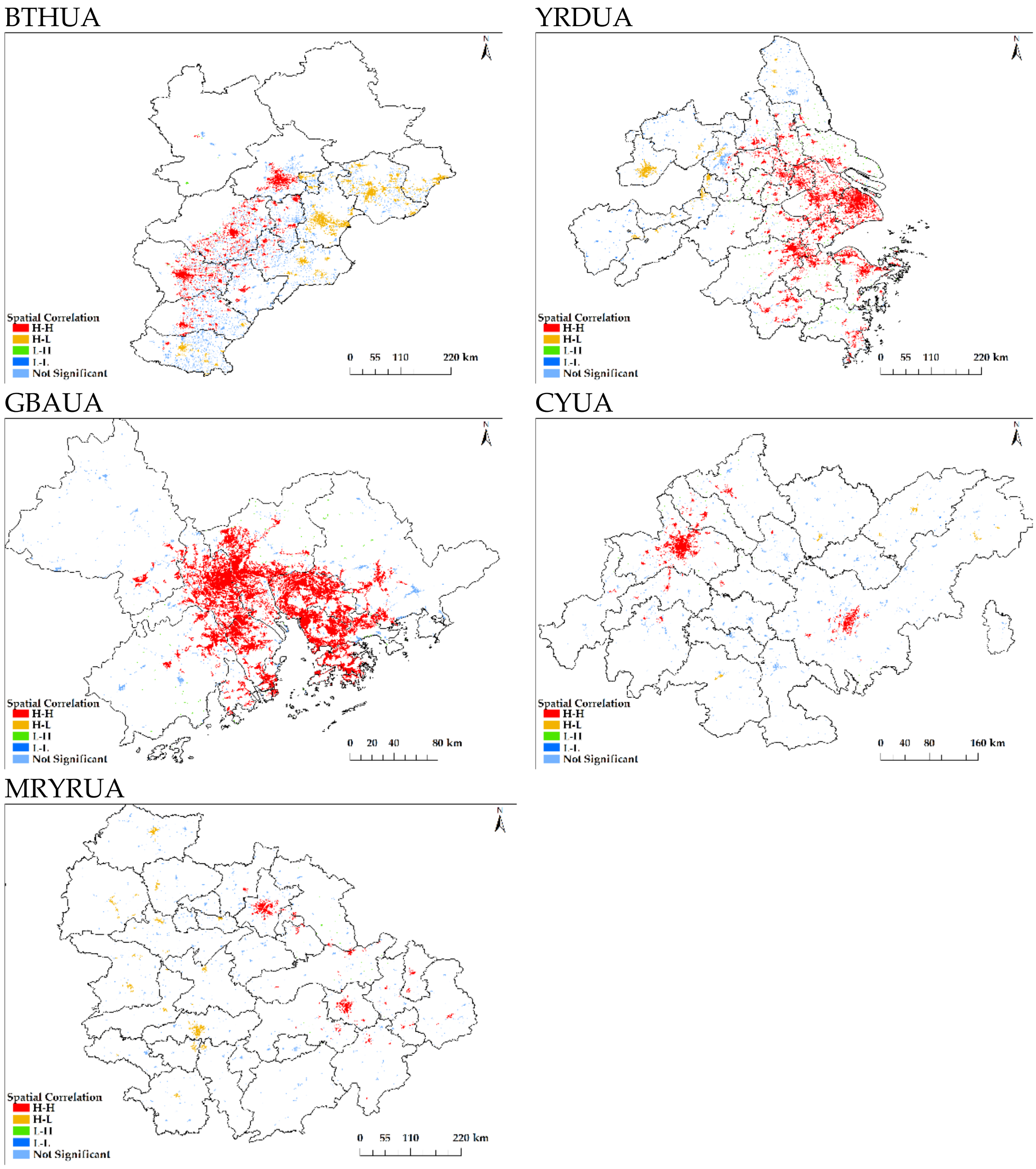

Figure 8. Cluster maps for local indicators of association (LISA) based on the weighted degree centrality of impervious surface areas.

Adding HH and HL can obtain the urbanization global high-potential area H, and adding LH and LL can obtain the urbanization global low-potential area L. Based on the percentages of spatial correlation classification, it can be derived that the percentage of area H in the five urban agglomerations is much higher than that of area L. The percentages of area H for GBAUA, YRDUA, BTHUA, CYUA, and MRYRUA decrease sequentially, at 0.90, 0.81, 0.69, 0.57, and 0.55, respectively (Figure 9). The percentages of area L for YRDUA, CYUA (MRYRUA), and BTHUA (GBAUA) decrease sequentially, at 0.07, 0.02, and 0.01, respectively. Furthermore, the siphoning areas HL with high potential show significant performance while the siphoned areas LH with lower potential are not significant. The percentages of area HL for BTHUA and MRYRUA are 0.28 and 0.21, respectively, while those for YRDUA, CYUA, and GBAUA are close to 0. The percentages of LH of BTHUA, GBAUA, CYUA, MRYRUA, and YRDUA are close to 0. Specifically, the first four are about 0.01, and the latter is 0.04. In general, the percentages of H and HL for the five urban agglomerations are far greater than those of L and LH, respectively. The former is greater than 55% and 21% while the latter are both close to 0.

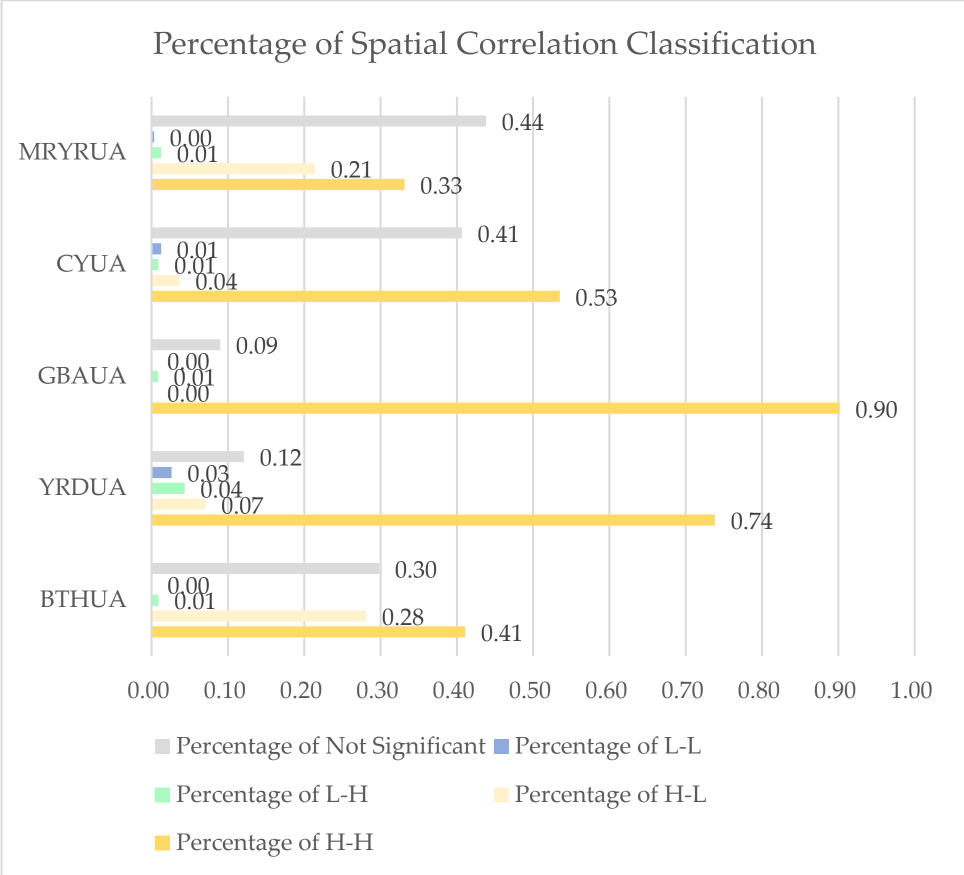

Figure 9. Area percentages of spatial correlation classification.

4.2.3. Analysis of Urban Agglomeration Corridors and Urban Agglomeration Connectivity

1. Extraction of Urban Agglomeration Corridors

The high connectivity of urban agglomeration corridors is the key to the balanced development of urban agglomerations, which is another important structure of urban agglomerations. In this study, the urban agglomeration corridors are generated based on the betweenness centrality of complex spatial networks (Figure 10). The size of the nodes shows the degree of mediation effect. The larger the nodes, the stronger the mediation effect. The main corridors of BTHUA are two northwest–southeast corridors, i.e., Beijing–Baoding–Shijiazhuang–Xingtai–Handan and Tangshan–Tianjin–Langfang–Cangzhou–Hengshui–Xingtai–Handan. Hub nodes in the two corridors are staggered in geographic space and form triangles through bridge nodes to connect and communicate. There are three main corridors in YRDUA, one west–southeast corridor, and two north–south corridors, i.e., Chuzhou–Nanjing–Zhenjiang–Changzhou–Suzhou–Shanghai, Anqing–Chizhou–Tongling–Wuhu–Ma'anshan–Xuancheng–Huzhou–Jiaxing, and Hefei–Nanjing–Changzhou–Wuxi–Jiaxing. The north–south corridor starts from Yancheng and is distributed into two east–west corridors, i.e., Yancheng–Yangzhou–Qinzhou–Zhenjiang–Changzhou–Wuxi–Huzhou–Jiaxing and Yancheng–Nantong–Suzhou–Shanghai–Jiaxing. The five urban agglomeration corridors are distributed into three channels in Jiaxing: Jiaxing–Shaoxing–Jinhua, Jiaxing–Shaoxing–Taizhou, and Jiaxing–Shaoxing–Ningbo. There are many corridors in the YRDUA, which can be roughly divided into northwest–southeast and north–south trends. There are three main routes in the northwest–southeast trends, i.e., Chuzhou–Nanjing–Zhenjiang–Changzhou–Suzhou–Shanghai, Anqing–Chizhou–Tongling–Wuhu–Ma'anshan–

Xuancheng–Huzhou–Jiaxing, and Hefei–Nanjing–Changzhou–Wuxi–Jiaxing. There are two main routes in the north–south direction, starting from Yancheng, and the distribution is divided into two east and west channels, i.e., Yancheng–Yangzhou–Qinzhou–Zhenjiang–Changzhou–Wuxi–Huzhou–Jiaxing and Yancheng–Nantong–Suzhou–Shanghai–Jiaxing. The GBAUA corridor is mainly composed of two ring-shaped corridors. The outer ring-shaped corridor is Huizhou–Dongguan–Guangzhou–Foshan–Jiangmen, and the inner ring-shaped corridor is Shenzhen–Dongguan–Zhongshan–Zhuhai. In CYUA, Chengdu and Chongqing are mainly connected by three main corridors from east to west. The first corridor is located in the northern part of CYUA, and it is composed of three sub-corridors, which from Mianyang, Deyang, and Chengdu converge to Suining and then distribute from Suining to Dazhou, Guang'an, and Chongqing. The second corridor is located in the middle of CYUA, and the key hub is Ya'an–Meishan–Neijiang–Chongqing. The third corridor is located in the south, which is Ya'an–Leshan–Yibin–Luzhou–Chongqing. The main corridors of MRYRUA are concentrated in its western region, and they are composed of north–south and east–west passages. The north–south urban corridor is Xiangfan–Jingmen–Tianmen–Qianjiang–Xantao–Jingzhou–Changde–Yueyang–Yiyang–Changsha, and the east–west corridor is Yichang–Qianjiang–Tianmen–Xantao–Wuhan–Ezhou–Huangshi. The eastern corridor is represented by two triangular components consisting of Jiujiang–Nanchang–Shangrao and Nanchang–Shangrao–Yingtan. To sum up, the results show that the corridors of BTHUA, YRDUA, and GBAUA have a high degree of integration, but there are giant corridor holes in the central part of CYUA and MRYRUA that reduce the connectivity between the east and the west.

2. Urban Agglomeration Connectivity Analysis

Urban agglomeration corridors reveal the connectivity of urban agglomerations. In order to quantify the connectivity, the numbers and proportion of connected components are calculated in this study (Table 3). The results show that BTHUA, YRDUA, GBAUA, and CYUA are all strongly connected, but MRYRUA is weakly connected. GBAUA has the least number of connected components, and the giant component's nodes account for more than 88%, indicating that there is strong connectivity in this region. MRYRUA has the largest number of connected components, and the giant component's nodes account for 53.78%, indicating that half of the nodes have insufficient connectivity. Combined with the spatial distribution of the connected components of MRYRUA (Figure 11), it can also be seen that there are mainly two connected components in MRYRUA, the east and the west, forming a spatial isolation, reflecting the low connectivity and correlation between the east and the west.

Table 3. Urban cluster connectivity indicators.

Urban Agglomerations	Number of Components	Largest Component/Percentage
BTHUA	23	12,471 vertices/96.205%
YRDUA	10	4396 vertices/99.098%
GBAUA	5	870 vertices/88.146%
CYUA	18	1663 vertices/95.192%
MRYRUA	51	1441 vertices/53.769%

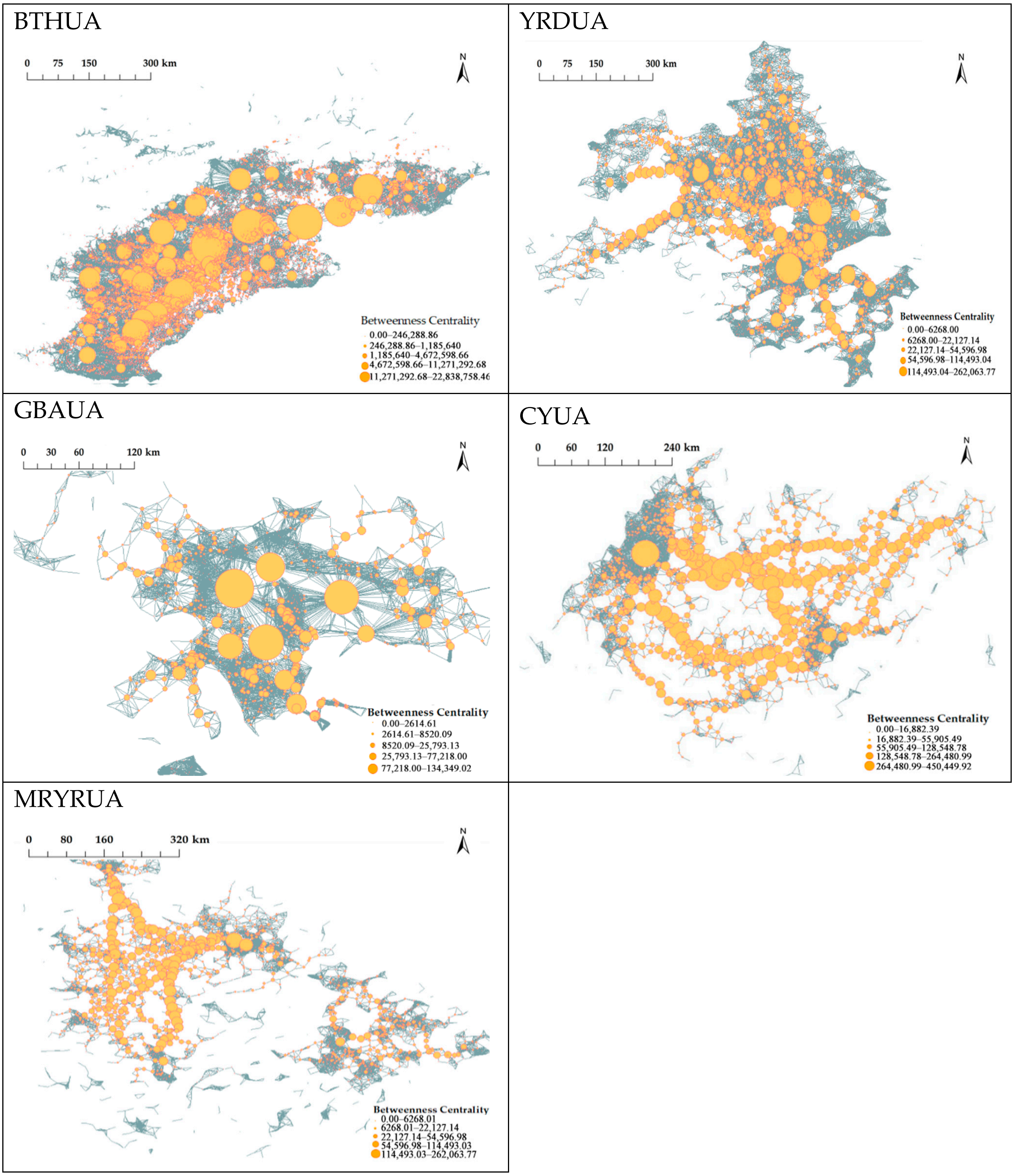

Figure 10. Spatial distribution of urban agglomeration corridors.

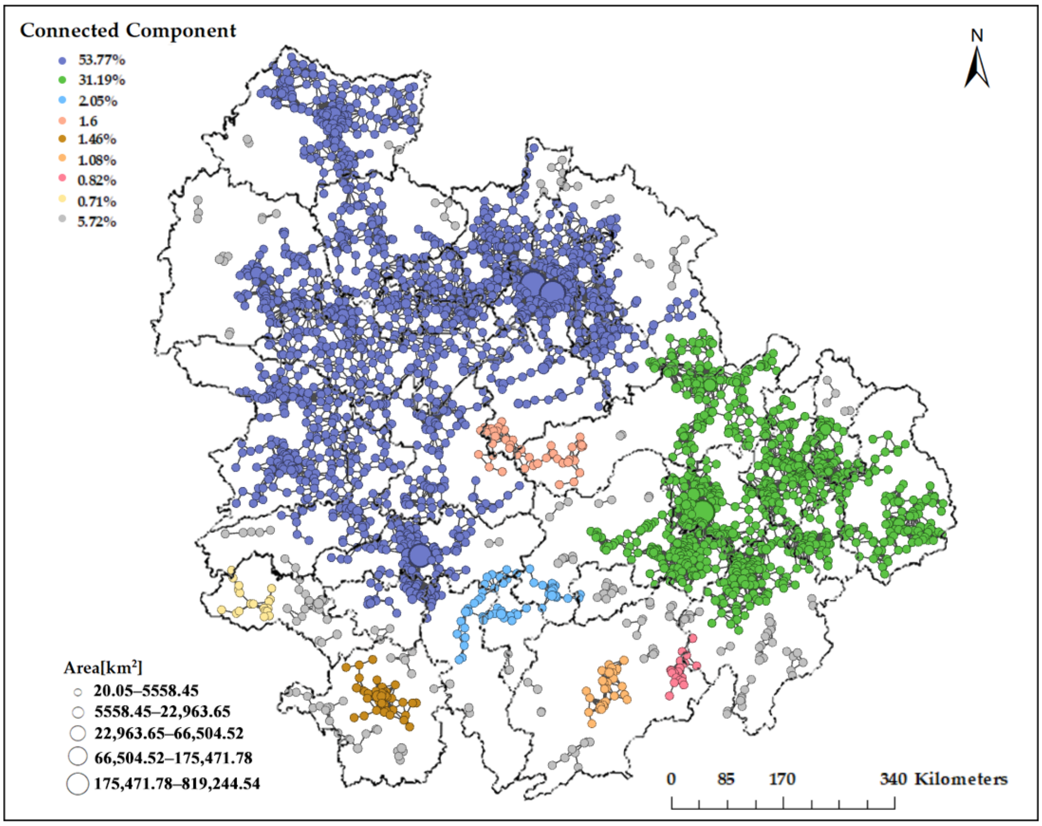

Figure 11. Spatial distributions of the connected components of MRYRUA.

4.2.4. Analysis of Regional Planning Differences Based on Spatial Pattern and Urbanization Potential Analysis Results

The purpose of this study is to explore the spatial pattern and development potential based on the internal spatial links of urban agglomeration networks and the spatial correlation between the links, so as to assist in the formulation of national and regional development planning; support the positive economic, social, and environmental links between urban, peri-urban/semi-dense areas, and rural areas; and achieve the effective monitoring of SDG11.A. Specifically, spatial links determine the spatial pattern, and the spatial correlation between the spatial links determines the development potential. The research results of spatial pattern and development potential provide baseline data and reference data for national and regional planning. Furthermore, the urbanization potential pattern, which is related to and different from the spatial pattern, drives the urban pattern development. Based on the above baseline data, this part provides a difference analysis for national and regional planning and consists of the following two parts.

1. The analysis of two connections; that is, the connections between the findings and the connections between the analyses. Three main findings were obtained in this study. First, the multi-centers and urban–rural continuum, which are the extraction and mapping of the global importance links of nodes in the urban agglomeration network. Second, the urban agglomeration corridor, which is the extraction and mapping of the global intermediary links of nodes. Third, the urbanization potential, which is the extraction and mapping of spatial aggregation patterns of global importance links. The analysis of the above two connections includes the following parts:
    (1) Multi-center planning analysis based on multi-centers and urbanization potential. It can be seen that the northwest of BTHUA, central CYUA, and central MRYRUA lack multi-centers, but high-potential areas appear in the areas, which can be planned as sub-centers in the next step, such as the urban area of Zhangjiakou in the northeast of BTHUA, the urban areas of Ziyang, Suining,

and Nanchong in the central CYUA, the northern urban area of Jiujiang, the southern urban area of Yichun, and the northern urban area of Yueyang in the central MRYRUA.

(2) The results of the comparative analysis of multi-centers and siphon effects show that the proportion of multi-centers with siphon effects of eastern urban agglomerations is higher than that in central and western urban agglomerations. Combined with the analysis of urban agglomeration corridors, the multi-centers with siphon effects also have a significant intermediary. In multi-center planning, the negative impact of the siphon effect should be reduced while maintaining the overall importance and intermediary of centers with negative impact. Specifically, siphon areas of BTHUA exist in three centers in the east—Tangshan, Tianjing, and Cangzhou—and one center in the south—Handan. The siphon area of YRDUA exists in the western center, Hefei. The siphon area of MRYRUA is located in the western center. However, the siphon area of GBAUA is not significant, and the siphon area of CYUA is located in the north non-central urban area.

(3) Combined with the analysis of multi-centers and urban agglomeration corridors it can be seen that multi-centers are the key nodes of urban agglomeration corridors, which have high intermediary centrality. It shows that the intermediary hub function is a prominent feature of multi-centers. Therefore, the urban agglomeration corridor provides more choices for multi-center planning. Although some hub nodes with relatively low urbanization potential values are far from the multi-centers, they can be planned as the sub-center to promote regional development based on the high intermediary centrality. For example, promoting the urban area of Yibin as the southern center and the urban areas of Dazhou and Nanchong as the northern center can fill the vacuum of multi-centers in the south and north of CYUA. Promoting Xiangfan, Yichang, Jingmen, Changde, Qiangjiang, and Jingzhou in the northwest of MRYRUA with high intermediary centrality and certain urbanization potential to be sub-centers can fill the vacancy of multi-centers in the northwest of MRYRUA. Combined with the analysis of the multi-centers and urbanization potential, the urban areas of Jiujiang and Yichun in the central MRYRUA will be determined again as the focus of the next multi-center planning.

(4) Regional planning analysis of the urban–rural continuum based on urban–rural continuum pattern and urbanization potential. The results show that the common ground of the five urban agglomerations is that the high-potential areas almost always appear in multi-centers and urban areas, and the low-potential areas appear in semi-dense areas and rural areas. It shows that there is a positive relationship between urbanization degree and potential. The difference between the five urban agglomerations is that the urban, semi-dense areas, and rural areas of GBAUA all show high urbanization potential. The reason is that GBAUA has reached a highly developed state with highly developed rural areas. Especially, the GDP of the district with a population of 1 million in GBAUA can reach nearly 300 billion, which is equal to the central provinces in China, such as Ningxia Province (http://static.nfapp.southcn.com/content/202112/27/c6076800.html, accessed on 28 November 2022).

Based on the comprehensive analysis of the above findings, regional planning should be conducted per the following points. First, policies should be formulated to promote the promotion and optimization of the above urbanization low-potential areas. Second, the siphon effect of the above siphoned areas should be used to cultivate the growth pole and then drive the overall development through the radiation effect and promotion effect. Last, for the construction of multi-center patterns, more sub-centers should be established according to the overall importance and intermediary.

2. National planning analysis based on the comparative analysis of the research results of the five major urban agglomerations. This section makes an overall comparative analysis of the five urban agglomerations from the connections between the degree of urbanization and the unbalanced development, the connections between the degree of urbanization and the potential, and the connections between the siphon effect, the degree of urbanization, and unbalanced development.

As can be seen from the above, the proportion of urban areas of GBAUA, YRDUA, BTHUA, CYUA, and MRYRUA decreased in turn, and the unbalanced development degree of YRDUA, CYUA, GBAUA, MRYRUA, and BTHUA decreased in turn. According to the research findings of urbanization degree and urban development balance, it can be seen that GBAUA has the highest degree of urbanization but ranks third in terms of unbalanced development, while YRDUA has the highest unbalanced development but ranks second in terms of urbanization. BTHUA and MRYRUA rank third and fifth in terms of urbanization but rank top two in terms of balanced development degree. CYUA ranks fourth in terms of urbanization but ranks second in terms of unbalanced development degree. This shows that the urbanization degree of China's current typical urban agglomerations is not positively related to the balance of urban development. In national planning, policies should be issued to continue to promote BTHUA's high score of urbanization and balanced development. The balanced development degree of MRYRUA is high, but the degree of urbanization should be strengthened. The urbanization performance of YRDUA is significant, but the unbalanced development degree of YRDUA should be reduced. CYUA's urbanization and balanced development scores are relatively low, and measures should be taken to better plan to promote urbanization and reduce unbalanced development.

In light of the five urban agglomerations ranking the same in terms of urbanization degree and potential, indicating that the degree of urbanization is related to the potential, areas with a high degree of urbanization usually have high potential. The comprehensive score of urbanization degree and potential of GBAUA, YRDUA, BTHUA, CYUA, and MRYRUA decreased in turn. It is worth noting that although YRDUA ranks second in terms of high urbanization potential, its proportion of low-potential areas is not the second from the bottom but the first. This result proves YRDUA's high degree of imbalance, which was obtained in the analysis in Section 4.2.2. In national urban planning, the potential degree of urbanization can be preliminarily deduced based on the current urbanization degree, which provides a basis for the layout and location selection of urban economic structure, spatial structure, and social structure.

The comprehensive analysis results of urbanization potential and siphon effect show that GBAUA has the highest proportion of high potential and the lowest proportion of siphon area, which proves that the imbalance of the urban development of GBAUA is relatively low, as was obtained in Section 4.2.2. The proportion of BTHUA and MRYRUA siphon areas is far higher than that of YRDUA and CYUA, and GBAUA has no siphon area. Based on the ranking results of unbalanced development, it is found that although the siphon effect of BTHUA and MRYRUA is significant, their balanced development scores are equal to YRDUA, indicating that the siphon areas with a small proportion is not the main factor affecting the balanced development of BTHUA and MRYRUA, and other global factors should be considered, such as policy, terrain, traffic patterns, etc.

5. Discussion

The research results of this paper on the muti-centers and the degree of urbanization of typical Chinese urban agglomerations are consistent with the results of China's 14th Five-Year Plan [63]. Referring to the GDP data released by the National Bureau of Statistics, the GDP rankings of Chinese cities in 2021 show the highly concentrated urban agglomeration muti-centers (http://static.nfapp.southcn.com/content/202112/27/c6076800.html, accessed on 28 November 2022). The top 10 cities are Shanghai, Beijing, Shenzhen, Guangzhou, Chongqing, Suzhou, Chengdu, Hangzhou, Wuhan, and Nanjing. The geographical distribution of this ranking is characterized by the prominent proportions of

BTHUA, YRDUA, and GBAUA. A total of 18 cities in the three urban agglomerations have entered the top 30 GDP rankings. Among them, Beijing, Shanghai, Suzhou, Hangzhou, Nanjing, Shenzhen, and Guangzhou, which are located in the three urban agglomerations, account for 17.4% of the country's total GDP, leading the first echelon of high-quality development. Chongqing and Chengdu of CYUA and Wuhan of MRYUA account for 5.7% of the country's total GDP and lead the second echelon of high-quality development. The results of the urbanization degree ranking and urban agglomeration multi-center spatial distribution obtained in this study are in good agreement with relevant government statistics, which proves the accuracy and reliability of this study.

From the perspective of the network scale (number of nodes and edges) of the five major urban agglomerations, BTHUA, YRDUA, MRYRUA, CYUA, and GBAUA decrease in order, which is mainly affected by the scope of the urban agglomeration, the area, and the pattern of impervious surfaces. Based on the analysis of the urban–rural continuum pattern, it can be seen that the number of multi-centers and the proportion of urban areas of the three urban agglomerations located in the eastern coastal areas of China are larger than those of the two urban agglomerations located in the mountainous regions of the central and western China. The factors affecting the patterns and unbalanced development of the five urban agglomerations are complex. This section mainly discusses the impacts of policies, topography, and transportation.

In terms of historical policies, the Chinese government has implemented the regional development strategies of "east lead, west development, revitalization of the northeast, rise of the central region" since the reform and opening up. In light of the eastern coastal region being convenient for international transportation, this area has the highest degree of opening to the outside world, and the highest degree of urbanization in China. It is also the region with the earliest formation and development of urban agglomerations.

One of the main reasons for the vacuum of muti-centers in the northwest of BTHUA, CYUA, and the middle of MRYRUA is the terrain and mountains. The terrain of China is high in the west and low in the east, with vast plains in the east and numerous mountains in the central and western regions. The barriers of the Taihang Mountains in the northwest of BTHUA, the Longquan Mountains in the southeast of Chengdu in CYUA, and the Luoxiao Mountains located at the junction of Hunan Province and Jiangxi Province in MRYRUA block the formation and connection of multi-centers. Thus, the northwest of BTHUA and central CYUA and MRYRUA are lacking multi-centers and corridors. The multi-center distribution of YRDUA and GBAUA is more balanced, mainly due to the flatness of the plain terrain without mountains barriers and with rich river–sea resources creating superior shipping conditions, which can help the balanced development of multi-core centers in urban agglomeration.

In addition, the accessibility of comprehensive transportation also leads to differences in the degree of urbanization and unbalanced development of the five urban agglomerations. At present, the comprehensive transportation system in the eastern region of China is basically formed, the central is accelerated, and the western region is still in the initial stage of development. The balanced development of the transportation system is an important factor affecting urban pattern development.

In terms of land transportation, the density of the transportation network of coastal urban agglomerations is significantly higher than that of inland mountainous urban agglomerations. Over-strengthening the traffic construction around large cities has led to the emergence of vacuum zones in central CYUA and MRYRUA [64], which is consistent with the research results of the urban agglomeration corridors in this study. The proportion of low-grade roads in the central and western urban agglomerations is higher than that in the eastern urban agglomerations, resulting in insufficient traffic capacity between core cities and slow urban development. Furthermore, most of the coastal urban agglomerations perform better than the central and western regions in terms of internal accessibility. This result is basically consistent with the research results of the urban agglomeration connectivity in Section 4.2.3. In general, the accessibility of land transportation is an important factor affecting urban development.

In terms of water transportation, the shipping data of the National Bureau of Statistics shows that the YRDUA and GBAUA are densely covered with river networks and numerous ports. In 2021, the cargo throughput of several ports of YRDUA, GBAUA, and BTHUA exceeded 100 million, respectively, while the throughput of ports in CYUA and MRYRUA was at the level of 10 million tons, with low-grade waterways resulting in poor long-distance transportation efficiency. Although the Yangtze River, the main waterway of China, passes through the southern part of CYUA and the northern part of MRYRUA, some of their waterway hubs are not smooth enough to connect with the Yangtze River, which affects traffic efficiency. However, the high overlapping rate of YRDUA's multi-center links and the Yangtze River waterway indicates the important influence of the waterway on the urban multi-center spatial construction.

In addition, air traffic is another important factor that promotes the formation of urban agglomeration centers, is less affected by terrain conditions, and can overcome the spatial obstacles caused by terrain, make up for the unbalanced development of the overall traffic system caused by the imbalance of land traffic and water traffic, and accelerate the efficiency of the formation of urban agglomeration centers. Air transport data from the National Bureau of Statistics of China show that air passenger traffic is highly concentrated in the five urban agglomerations and central cities, and the trend of air cargo concentrating in central cities is more significant. In 2021, among the top ten cities with the largest airport passenger throughput in China, the top eight are all the five major urban agglomeration centers (https://www.mot.gov.cn/tongjishuju/minhang/202204/t20220408_3649981.html, accessed on 28 November 2022).

In general, CYUA and MRYRUA are limited by their mountain topography, which affects the establishment of a comprehensive transportation network and hinders the formation of multi-centers and urban areas. Therefore, the number of multi-centers and the proportion of urban areas is lower than BTHUA, YRDUA, and GBAUA.

Based on the research results, to facilitate the monitoring of SDG11.A "support positive economic, social and environmental links between urban, peri-urban and rural areas by strengthening national and regional development planning", the recommendations for urban agglomeration planning are as follows:

1. The research results can be used as reference data, and areas with high urbanization potential and strong intermediary hub functions can be planed as sub-centers and micro-centers.
2. Policies should be adopted to promote the transformation of areas with strong siphon effects into spillover effects and promote overall development through "radiation effects", "promoting effects", and "chain effects" to reduce the negative impact of siphons.
3. Comprehensive transportation systems with the coordinated development of water transportation, land transportation, and air transportation should be established to eliminate the imbalance in urban development caused by the imbalance in the transportation network.

This study is innovative in both methodology and data. The innovation of the monitoring methods of SDG11.A can be summarized as the combination of a complex spatial network and remote sensing technology to fully mine two spatial relationships, namely the spatial links and the spatial correlation of spatial links. The usual urban network research mainly extracts spatial links without mining the spatial aggregation patterns of spatial links to further analyze urbanization potential, such as the study of European urban networks [54]. In terms of data innovation, research on urban links is usually based on statistical data such as socio-economic data, demographic data, and social dynamic flow data. However, due to the low spatial and temporal resolution, these data usually are not easy to decompose into corresponding research scales and cannot flexibly and completely describe the links between regions and map the spatial patterns. However, the research scale of this study is not limited by the Hi-GISA data with high-precision and a global spatial resolution of 10 m, and it can be flexibly applied to urbanization research at multi-scales. The local information can also be considered and mined in large-scale research, which can achieve a complete description of regional spatial links.

In the future, further research can be conducted on the selection of buffer radius thresholds, the setting of classification thresholds for urban agglomeration patterns, and the verification of classification results. Multiple groups of comparison experiments with different buffer radii should be conducted to analyze the differences in results. Furthermore, the classification threshold setting should be combined with the verification of classification results to obtain the optimal classification threshold.

6. Conclusions

Although there are many urbanization studies based on satellite-derived products of global impervious surface area or human settlements, the large-scale spatial correlation analysis of urban agglomerations is rarely mentioned. Based on the self-developed global 10 m high-precision impervious surface product Hi-GISA 2021, this study combined the complex network with remote sensing technology to build the complex spatial network model of urban agglomerations. The spatial links and the spatial correlation of the spatial links were extracted to analyze the patterns and the potential for urbanization. Specifically, the multi-centers, urban–rural continuum, urban agglomeration corridors, and urbanization potential areas of BTHUA, YRDUA, GBAUA, CYUA, and MRYRUA were extracted and analyzed. The results can accurately assess the urbanization development status of these urban agglomerations, as well as provide data, methods, and technical support for monitoring and evaluating SDG11.A "support positive economic, social and environmental links between urban, peri-urban and rural areas by strengthening national and regional development planning". The results show the diversity of the urbanization process of the five typical Chinese urban agglomerations. First, BTHUA, YRDUA, GBAUA, CYUA, and MRYRUA are all small-world networks with a low degree of overall polycentricity; the urbanization degrees of GBAUA and YRDUA are higher than BTHUA, CYUA, and MRYRUA; and the spatial distribution of the multi-centers, the urban–rural continuum, and the agglomeration corridors are strikingly different in each urban agglomeration. Second, the imbalanced development of YRDUA is higher than the other regions, and the siphon effects of BTHUA and MRYRUA are more significant than YRDUA, CYUA, and GBAUA. Third, multi-centers have high global importance and intermediary effects, and some of them show significant siphon effects. Last, the urbanization degree of China's typical urban agglomerations is highly correlated with the urbanization potential but not positively correlated with the degree of balanced development. The siphon area with a low proportion is not the main factor affecting the overall balanced development of urban agglomerations.

Nonetheless, there are still some limitations to this study, even though, compared with the officially released urban agglomeration multi-centers in China [63], the extraction results in this study are objective and accurate. Future work will be focused on the systematic validation and optimization of net pattern classifications. Furthermore, it is important to thoroughly investigate the relationships and interdependencies between the model's evaluation indicators and parameter settings (e.g., search buffers). In the meanwhile, the long-term observation and evaluation of spatial correlation and differentiation of typical global urban agglomerations from the perspective of horizontal and vertical expansion should be included in future work. It will also be necessary to classify spatial patterns according to state-of-the-art concepts and theories in urban planning. In order to better evaluate SDG 11, these factors need to be taken into account in future studies.

Author Contributions: Conceptualization Z.S.; methodology, S.L. and Z.S.; formal analysis, S.L.; writing—original draft preparation, S.L.; writing—review and editing, Z.S., Z.L., H.J. and H.Z.; supervision, H.G.; funding acquisition, H.G. and Z.S. All authors have read and agreed to the published version of the manuscript.

Funding: This research was funded by the Key R&D Program Projects in Hainan Province (Grant No. ZDYF2020192), National Natural Science Foundation of China (Grant No. 42171291), Innovative Research Program of the International Research Center of Big Data for Sustainable Development Goals (Grant No. CBAS2022IRP04), and Key R&D Program of Guangxi (Grant No. Guike-AB22035060).

Data Availability Statement: The data presented in this study are available on request from the corresponding author.

Acknowledgments: We appreciate the critical and constructive comments and suggestions from the reviewers that helped improve the quality of this manuscript.

Conflicts of Interest: The authors declare no conflict of interest.

References

1. Guo, H.; Chen, F.; Sun, Z.; Liu, J.; Liang, D. Big Earth Data: A practice of sustainability science to achieve the Sustainable Development Goals. *Sci. Bull.* **2021**, *66*, 1050–1053. [CrossRef] [PubMed]
2. Guo, H.; Liang, D.; Sun, Z.; Chen, F.; Wang, X.; Li, J.; Zhu, L.; Bian, J.; Wei, Y.; Huang, L.; et al. Measuring and evaluating SDG indicators with Big Earth Data. *Sci. Bull.* **2022**, *67*, 1792–1801. [CrossRef]
3. UN. *Transforming Our World: The 2030 Agenda for Sustainable Development*; United Nations: New York, NY, USA, 2016.
4. UN Department of Economic and Social Affairs Population Division. *The World's Cities in 2018—Data Booklet (ST/ESA/SER.A/417)*; UN Department of Economic and Social Affairs Population Division: New York, NY, USA, 2018.
5. Jiang, H.; Sun, Z.; Guo, H.; Weng, Q.; Du, W.; Xing, Q.; Cai, G. An assessment of urbanization sustainability in China between 1990 and 2015 using land use efficiency indicators. *npj Urban Sustain.* **2021**, *1*, 34. [CrossRef]
6. Jiang, H.; Guo, H.; Sun, Z.; Xing, Q.; Zhang, H.; Ma, Y.; Li, S. Projections of urban built-up area expansion and urbanization sustainability in China's cities through 2030. *J. Clean. Prod.* **2022**, *367*, 133086. [CrossRef]
7. UN Department of Economic and Social Affairs Population Division. *World Urbanization Prospects: The 2018 Revision*; UN Department of Economic and Social Affairs Population Division: New York, NY, USA, 2018.
8. Dye, C. Health and urban living. *Science* **2008**, *319*, 766–769. [CrossRef] [PubMed]
9. Seto, K.C.; Fragkias, M.; Güneralp, B.; Reilly, M.K. A meta-analysis of global urban land expansion. *PLoS ONE* **2011**, *6*, e23777.
10. UN Habitat. *World Cities Report 2022: Envisaging the Future of Cities*; UN Habitat: Nairobi, Kenya, 2022.
11. Zhou, Y.; He, X.; Zhu, Y. Identification and Evaluation of the Polycentric Urban Structure: An Empirical Analysis Based on Multi-Source Big Data Fusion. *Remote Sens.* **2022**, *14*, 2705.
12. Fang, C.; Yu, X.; Zhang, X.; Fang, J.; Liu, H. Big data analysis on the spatial networks of urban agglomeration. *Cities* **2020**, *102*, 102735. [CrossRef]
13. Phillips, J.D.; Schwanghart, W.; Heckmann, T. Graph theory in the geosciences. *Earth-Sci. Rev.* **2015**, *143*, 147–160.
14. Castells, M. *The Rise of the Network Society*; Blackwell: Cambridge, MA, USA, 2006.
15. Leng, B.R.; Yang, Y.C.; Li, Y.J.; Zhao, S. Spatial characteristics and complex analysis: A perspective from basic activities of urban networks in China. *Acta Geogr. Sin.* **2011**, *66*, 199–211.
16. Li, Y.C. A preliminary analysis on urban innovation network of metropolitan region and its characteristics. *Plan. Stud.* **2019**, *43*, 27–33, 39.
17. Taylor, P.J. Urban hinterworlds: Geographies of corporate service provision under conditions of contemporary globalisation. *Geography* **2001**, *86*, 51–60.
18. Taylor, P.J.; Catalano, G.; Walker, D.R.F. Measurement of the world city network. *Urban Stud.* **2002**, *39*, 2367–2376. [CrossRef]
19. Taylor, P.J. Leading world cities: Empirical evaluations of urban nodes in multiple networks. *Urban Stud.* **2005**, *42*, 1593–1608. [CrossRef]
20. Matthiessen, C.W.; Schwarz, A.W.; Find, S. World cities of scientific knowledge: Systems, networks and potential dynamics. An analysis based on bibliometric indicators. *Urban Stud.* **2010**, *47*, 1879–1897. [CrossRef]
21. Wang, L.; Duan, X. High-speed rail network development and winner and loser cities in megaregions: The case study of Yangtze River Delta, China. *Cities* **2018**, *83*, 71–82.
22. Yeh, A.G.O.; Yang, F.F.; Wang, J.J. Producer service linkages and city connectivity in the mega-city region of China: A case study of the Pearl River Delta. *Urban Stud.* **2015**, *52*, 2458–2482.
23. Pan, F.H.; Bi, W.K.; Lenzer, J.; Zhao, S. Mapping urban networks through inter-firm service relationships: The case of China. *Urban Stud.* **2017**, *54*, 3639–3654.
24. Zhang, X.; Wang, X.; Zhang, C.; Zhai, J. Development of a cross-scale landscape infrastructure network guided by the new Jiangnan watertown urbanism: A case study of the ecological green integration demonstration zone in the Yangtze River Delta, China. *Ecol. Indic.* **2022**, *143*, 109317.
25. Zhao, S.-M.; Ma, Y.-F.; Wang, J.-L.; You, X.-Y. Landscape pattern analysis and ecological network planning of Tianjin City. *Urban For. Urban Green.* **2019**, *46*, 126479.
26. Simone, A.; Ciliberti, F.G.; Laucelli, D.B.; Berardi, L.; Giustolisi, O. Edge betweenness for water distribution networks domain analysis. *J. Hydroinform.* **2020**, *22*, 121–131. [CrossRef]

27. Naufan, I.; Sivakumar, B.; Woldemeskel, F.M.; Raghavan, S.V.; Vu, M.T.; Liong, S.-Y. Spatial connections in regional climate model rainfall outputs at different temporal scales: Application of network theory. *J. Hydrol.* **2018**, *556*, 1232–1243. [CrossRef]
28. Narayanan, B.L.; Yosri, A.; Ezzeldin, M.; El-Dakhakhni, W.; Dickson-Anderson, S. A complex network theoretic approach for interdependence investigation: An application to radionuclide behavior in the subsurface. *Comput. Geosci.* **2021**, *157*, 104913. [CrossRef]
29. Wu, C.-L.; Wang, H.-W.; Cai, W.-J.; Ni, A.-N.; Peng, Z.-R. Impact of the COVID-19 lockdown on roadside traffic-related air pollution in Shanghai, China. *Build. Environ.* **2021**, *194*, 107718. [CrossRef]
30. Rehman, A.U.; Singh, R.; Praveen, A. Modeling, analysis and prediction of new variants of COVID-19 and dengue co-infection on complex network. *Chaos Solitons Fractals* **2021**, *150*, 111008. [CrossRef]
31. Cai, K.-Q.; Zhang, J.; Du, W.; Cao, X. Analysis of the Chinese air route network as a complex network. *Chin. Phys. B* **2012**, *21*, 028903. [CrossRef]
32. Li, W.; Deng, L.; Liu, P.; Fan, Y.; Wang, J.; Sha, X.; Kong, X. A Monte Carlo simulation model of epidemic problem incorporating the interplaying between the crowd panic and infectious disease. *Mod. Phys. Lett. B* **2021**, *35*, 2150394. [CrossRef]
33. Zhang, W.; Bai, S.Y.; Jin, R. The model of microblog message diffusion based on complex social network. *Int. J. Mod. Phys. B* **2014**, *28*, 1450136. [CrossRef]
34. Najafi, M.N.; Rahimi-Majd, M.; Shirzad, T. Avalanches on the complex network of Rigan earthquake. *Europhys. Lett.* **2020**, *130*, 20001. [CrossRef]
35. Tobler, W.R. A computer movie simulating urban growth in the Detroit region. *Econ. Geogr.* **1970**, *46*, 234–240. [CrossRef]
36. He, Q.; He, W.; Song, Y.; Wu, J.; Yin, C.; Mou, Y. The impact of urban growth patterns on urban vitality in newly built-up areas based on an association rules analysis using geographical 'big data'. *Land Use Policy* **2018**, *78*, 726–738. [CrossRef]
37. Xu, C.; Liu, M.; Zhang, C.; An, S.; Yu, W.; Chen, J.M. The spatiotemporal dynamics of rapid urban growth in the Nanjing metropolitan region of China. *Landsc. Ecol.* **2007**, *22*, 925–937. [CrossRef]
38. Pham, H.M.; Yamaguchi, Y. Urban growth and change analysis using remote sensing and spatial metrics from 1975 to 2003 for Hanoi, Vietnam. *Int. J. Remote Sens.* **2011**, *32*, 1901–1915. [CrossRef]
39. Mahtta, R.; Mahendra, A.; Seto, K.C. Building up or spreading out? Typologies of urban growth across 478 cities of 1 million+. *Environ. Res. Lett.* **2019**, *14*, 124077. [CrossRef]
40. Cliff, A.; Ord, J.K. *Spatial Autocorrelation*; Pion: London, UK, 1973.
41. Haining, R.P. *Spatial Data Analysis: Theory and Practice*; Cambridge University: Cambridge, UK, 2003.
42. Anselin, L. Local indicators of spatial association (LISA). *Geogr. Anal.* **1995**, *27*, 93–115. [CrossRef]
43. Ray, B.; Glenn, D.; Stuart, K.; William, J.S. A comparison of the 1998 and 2002 coral bleaching events on the Great Barrier Reef: Spatial correlation, patterns, and predictions. *Coral Reefs* **2004**, *23*, 74–83.
44. Wang, W.Q.; Ying, Y.Y.; Wu, Q.Y.; Zhang, H.P.; Ma, D.D.; Xiao, W. A GIS-based spatial correlation analysis for ambient air pollution and AECOPD hospitalizations in Jinan, China. *Respir. Med.* **2015**, *109*, 372–378. [CrossRef] [PubMed]
45. Janssen, M.E.; Stephenson, R.A.; Cloetingh, S. Temporal and spatial correlations between changes in plate motions and the evolution of rifted basins in Africa. *GSA Bull.* **1995**, *10*, 1317–1332. [CrossRef]
46. Roxane, F.P.; Peter, J.S. A predictive model for Arias intensity at multiple sites and consideration of spatial correlations. *Earthq. Eng. Struct. Dyn.* **2012**, *41*, 431–451.
47. Cao, H.; Mamoulis, N.; Cheung, D.W. Mining frequent spatio-temporal sequential patterns. In Proceedings of the Fifth IEEE International Conference on Data Mining, Houston, TX, USA, 27–30 November 2005.
48. Giannotti, F.; Nanni, M.; Pedreschi, D.; Pinelli, F.; Renso, C.; Rinzivillo, S.; Trasarti, R. Unveiling the complexity of human mobility by querying and mining massive trajectory data. *VLDB J.* **2011**, *20*, 695–719. [CrossRef]
49. Trasarti, R.; Olteanu, R.; Olteanu-Raimond, A.-M.; Nanni, M.; Couronné, T.; Furletti, B.; Giannotti, F.; Smoreda, Z.; Ziemlicki, C. Discovering urban and country dynamics from mobile phone data with spatial correlation patterns. *Telecommun. Policy* **2015**, *39*, 347–362. [CrossRef]
50. Horton, F.E.; Reynolds, D.R. Effects of urban spatial structure on individual behavior. *Econ. Geogr.* **1971**, *47*, 36–48. [CrossRef]
51. Wang, Y.; Shen, Z. Comparing luojia 1-01 and viirs nighttime light data in detecting urban spatial structure using a threshold-based kernel density estimation. *Remote Sens.* **2021**, *13*, 1574. [CrossRef]
52. Sun, Z.; Yu, S.; Guo, H.; Wang, C.; Zhang, Z.; Xu, R. Assessing 40 years of spatial dynamics and patterns in megacities along the Belt and Road region using satellite imagery. *Int. J. Digit. Earth* **2020**, *14*, 71–87. [CrossRef]
53. Sun, Z.; Du, W.; Jiang, H.; Weng, Q.; Guo, H.; Han, Y.; Xing, Q.; Ma, Y. Global 10-m impervious surface area mapping: A big earth data based extraction and updating approach. *Int. J. Appl. Earth Obs. Geoinf.* **2022**, *109*, 102800. [CrossRef]
54. Esch, T.; Marconcini, M.; Marmanis, D.; Zeidler, J.; Elsayed, S.; Metz, A.; Müller, A.; Dech, S. Dimensioning urbanization–An advanced procedure for characterizing human settlement properties and patterns using spatial network analysis. *Appl. Geogr.* **2014**, *55*, 212–228. [CrossRef]
55. Jiang, H.; Sun, Z.; Guo, H.; Xing, Q.; Du, W.; Cai, G. A Standardized Dataset of Built-up Areas of China's Cities with Populations over 300,000 for the Period 1990–2015. *Big Earth Data* **2022**, *6*, 103–126. [CrossRef]
56. Franco, D.G.d.B.; Steiner, M.T.A.; Assef, F.M. Optimization in waste landfilling partitioning in Paraná State, Brazil. *J. Clean. Prod.* **2021**, *283*, 125353. [CrossRef]

57. Newman, M.E. Scientific collaboration networks. II. Shortest paths, weighted networks, and centrality. *Phys. Rev. E* **2001**, *64*, 016132. [CrossRef] [PubMed]
58. Watts, D.J.; Strogatz, S.H. Collective dynamics of 'small-world' networks. *Nature* **1998**, *393*, 440–442. [CrossRef] [PubMed]
59. Tiefelsdorf, M.; Boots, B. A note on the extremities of local Moran's Iis and their impact on global Moran's I. *Geogr. Anal.* **1997**, *29*, 248–257. [CrossRef]
60. Bivand, R.; Müller, W.G.; Reder, M. Power calculations for global and local Moran's I. *Comput. Stat. Data Anal.* **2009**, *53*, 2859–2872. [CrossRef]
61. UN Habitat. *SDG GOAL 11 Monitoring Framework: A Guide to Assist National and Local Governments to Monitor and Report on SDG Goal 11 Indicators*; UN Habitat: Nairobi, Kenya, 2016.
62. Chen, Z.; Yu, B.; Song, W.; Liu, H.; Wu, Q.; Shi, K.; Wu, J. A new approach for detecting urban centers and their spatial structure with nighttime light remote sensing. *IEEE Trans. Geosci. Remote Sens.* **2017**, *55*, 6305–6319. [CrossRef]
63. Central People's Government of the People's Republic of China. Available online: http://www.gov.cn/xinwen/2021-03/13/content_5592681.html (accessed on 12 October 2022).
64. Huang, Y.; Zong, H.M.; Luo, S.C.; Yi, Z. Comparative Study on the Spatial Pattern and Accessibility of Overland Transportation Network in China's Super-Large Urban Agglomerations. *Mod. Urban Res.* **2019**, *4*, 24–32.